Analog Modulation

Angle modulation

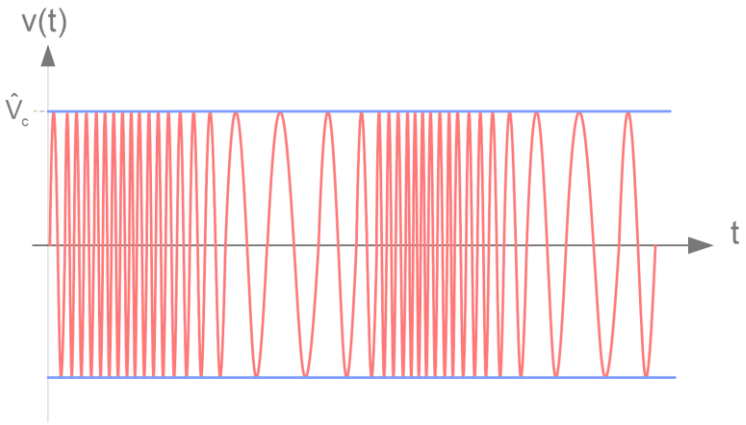

FM Frequency modulation

PM Phase modulation

Content

2.2 Angle modulation

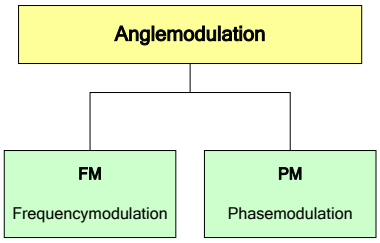

Fig. 2-1: Variants of angle modulations

2.2.1 Frequency and Phase Modulation

Frequency modulation:

The instantaneous frequency of carrier $\omega_c(t)$ is influenced by the modulation content:

$$\omega_c(t) = f\left(v_m(t)\right) \tag{2.1}$$

Phase modulation:

The instantaneous phase of the carrier $\varphi_c(t)$ is influenced by the modulation content:

$$\varphi_c(t) = f\left(v_m(t)\right) \tag{2.2}$$

Frequency and phase of a harmonic carrier are contained in the argument (angle) of the cosine function. Both frequency and phase modulation influence the angle. They are therefore subsumed under the term **Angle Modulation**.

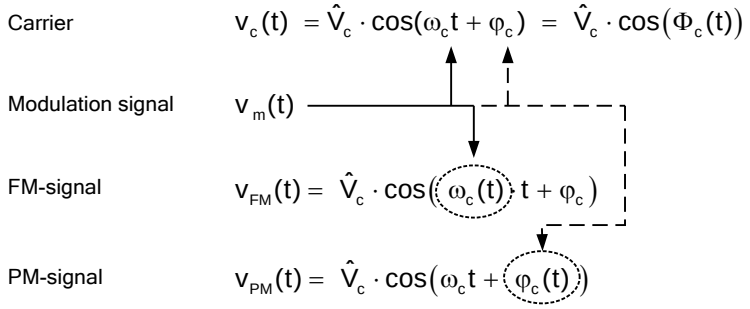

(2.3)

Hence, the angle $\Phi_c(t)$ of the carrier, which is already subject to time when it is not modulated, is additionally influenced by the modulation signal. The carrier amplitude $\hat{V}_c$ always remains constant.

For the purpose of examination, a sinusoidal signal is used for the modulation signal as well:

$$v_m(t) = \hat{V}_m \cos(\omega_m t) \tag{2.4}$$

The angle-modulated signal will be

$$v_{PM}(t) = \hat{V}_c \cos\left(\varphi_{PM}(t)\right) \tag{2.5}$$

The entire instantaneous phase $\varphi_{PM}(t)$ is the sum of the carrier's instantaneous phase $\varphi_c(t) = \omega_c t$ and the instantaneous phase $\varphi_m(t)$, which is generated by the modulation signal.

$$\varphi_{PM}(t) = \varphi_c(t) + \varphi_m(t) \tag{2.6}$$

$$\varphi_m(t) = \Delta\varphi_c \cos(\omega_m t) \tag{2.7}$$

In this case, $\Delta\varphi_c$ is the maximum phase difference between the modulated and the unmodulated carrier. $\Delta\varphi_c$ is designated as phase deviation or modulation index η.

$$\varphi_{PM}(t) = \omega_c t + \Delta\varphi_c \cos(\omega_m t) \tag{2.8}$$

Hence, the time function of the angle-modulated carrier will be

$$v_{PM}(t) = \hat{V}_c \cos\left[\omega_c t + \Delta\varphi_c \cos(\omega_m t)\right] = \hat{V}_c \cos\left[\omega_c t + \eta\cos(\omega_m t)\right] \tag{2.9}$$

From the instantaneous phase $\varphi_{PM}(t)$, the instantaneous angular frequency of the modulated carrier can be determined by way of differentiation:

$$\omega_{PM}(t) = \frac{d\varphi_{PM}(t)}{dt} = \omega_c - \Delta\varphi_c \omega_m \sin(\omega_m t) \tag{2.10}$$

The instantaneous frequency of the modulated carrier can be determined with $\Delta\varphi_c \omega_m = \Delta\omega_c$

$$f_{PM(t)} = \frac{\omega_{PM}(t)}{2\pi} = f_c - \Delta f_c \sin(\omega_m t) \tag{2.11}$$

The frequency deviation $\Delta f_c = \Delta\varphi_c f_m = \eta \cdot f_m$ is the maximum frequency difference between the modulated and the unmodulated carrier.

For the modulation index η, the following applies:

$$\eta = \Delta\varphi_c = \frac{\Delta f_c}{f_m} \tag{2.12}$$

From the equation (2.9) the time function of the frequency-modulated carrier can be described

$$v_{FM}(t) = \hat{V}_c \cdot \cos\left(\omega_c t + \frac{\Delta f_c}{f_m}\cos(\omega_m t)\right) \tag{2.13}$$

The equations (2.9) and (2.13) show that if the modulation frequency is constant, phase and frequency modulation cannot be distinguished.

Spectrum of Angle modulation

For the spectrum analysis, the Fourier coefficients must be determined. For this purpose, the equation (2.9) is represented as a complex equation:

$$v_{PM}(t) = \hat{V}_c \cos\left[\omega_c t + \eta\cos(\omega_m t)\right] = \hat{V}_c \cdot \mathrm{Re}\left(e^{j(\omega_c t + \eta\cdot\cos(\omega_m t))}\right) = \hat{V}_c \cdot \mathrm{Re}\left(e^{j\omega_c t} \cdot e^{j\eta\cdot\cos(\omega_m t)}\right) \tag{2.14}$$

With the power series $e^x = 1 + \frac{x}{1!} + \frac{x^2}{2!} + \frac{x^3}{3!} + \ldots + \frac{x^n}{n!} + \ldots$ and $x = j\eta\cos(\omega_m t)$,

the factor $e^{j\eta\cdot\cos(\omega_m t)}$ can be represented as follows:

$$\begin{aligned} e^{j\eta\cdot\cos(\omega_m t)} &= 1 + j\eta\cdot\cos(\omega_m t) + \frac{1}{2!}j^2\eta^2\cos^2(\omega_m t) + \frac{1}{3!}j^3\eta^3\cos^3(\omega_m t) + \ \ldots \\ &= 1 + j\eta\cdot\cos(\omega_m t) + \frac{1}{2!}j^2\eta^2\frac{1}{2}\left[1+\cos(2\omega_m t)\right] + \frac{1}{3!}j^3\eta^3\frac{1}{4}\left[\cos(3\omega_m t)+\cos(\omega_m t)\right] \\ &\quad + \frac{1}{4!}j^4\eta^4\frac{1}{8}\left[\cos(3\omega_m t) + 4\cos(2\omega_m t) + 3\right] + \ \ldots \end{aligned} \tag{2.15}$$

Sorted according to frequencies:

$$\begin{aligned} e^{j\eta\cdot\cos(\omega_m t)} &= \underbrace{\left[1 - \left(\frac{\eta}{2}\right)^2 + \frac{1}{4}\left(\frac{\eta}{2}\right)^4 - \frac{1}{36}\left(\frac{\eta}{2}\right)^6 + \ldots\right]}_{J_0(\eta)} \\ &\quad + 2j\underbrace{\left[\left(\frac{\eta}{2}\right) - \frac{1}{2}\left(\frac{\eta}{2}\right)^3 + \frac{1}{12}\left(\frac{\eta}{2}\right)^5 - \ldots\right]}_{J_1(\eta)}\cos(\omega_m t) \\ &\quad + 2j^2\underbrace{\left[\frac{1}{2}\left(\frac{\eta}{2}\right)^2 - \frac{1}{6}\left(\frac{\eta}{2}\right)^4 + \frac{1}{48}\left(\frac{\eta}{2}\right)^6 - \ldots\right]}_{J_2(\eta)}\cos(2\omega_m t) \\ &\quad + 2j^3\underbrace{\left[\frac{1}{6}\left(\frac{\eta}{2}\right)^3 - \frac{1}{24}\left(\frac{\eta}{2}\right)^5 + \frac{1}{240}\left(\frac{\eta}{2}\right)^6 - \ldots\right]}_{J_3(\eta)}\cos(3\omega_m t) \end{aligned} \tag{2.16}$$

$$e^{j\eta\cdot\cos(\omega_m t)} = J_0(\eta) + 2j\cdot J_1(\eta)\cdot\cos(\omega_m t) + 2j^2\cdot J_2(\eta)\cdot\cos(2\omega_m t) + 2j^3\cdot J_3(\eta)\cdot\cos(3\omega_m t) + \ \ldots \tag{2.17}$$

$J_n(\eta)$ are designated as Bessel functions of the first kind of order n (n = 0, 1, 2, 3, ...). Their function values can be found in diagrams or tables or they can be calculated numerically.

The following applies to the representation as a series:

$$J_n(\eta) = \sum_{k=0}^{\infty}\frac{(-1)^k\left(\frac{\eta}{2}\right)^{n+2k}}{k!(n+k)!} \tag{2.18}$$

If the function values for $n = 0$ and $n = 1$ are known, the Bessel functions for $n \geq 2$ can be calculated iteratively:

$$J_n(\eta) = \frac{2(n-1)}{\eta}J_{n-1}(\eta) - J_{n-2}(\eta) \tag{2.19}$$

In addition, the following applies to the Bessel functions:

$$J_{-n}(\eta) = (-1)^n J_n(\eta) \qquad |J_{-n}(\eta)| = |J_n(\eta)| \tag{2.20}$$

The new term for $e^{j\eta\cdot\cos(\omega_m t)}$ can now be inserted in the equation for $v_{PM}(t)$. Subsequently, the real part must be formed:

$$\begin{aligned} v_{PM}(t) &= \hat{V}_c \cdot \mathrm{Re}\left(e^{j\omega_c t}\cdot e^{j\eta\cdot\cos(\omega_m t)}\right) = \hat{V}_c \cdot \mathrm{Re}\left[(\cos(\omega_c t) - j\sin(\omega_c t))\cdot e^{j\eta\cdot\cos(\omega_m t)}\right] \\ &= \hat{U}_c \cdot \{[J_0(\eta) - 2\cdot J_2(\eta)\cdot\cos(2\omega_m t) + \ldots]\cdot\cos(\omega_c t) \\ &\quad - [2\cdot J_1(\eta)\cdot\cos(\omega_m t) - 2\cdot J_3(\eta)\cdot\cos(3\omega_m t) + \ldots]\cdot\sin(\omega_c t)\} \end{aligned} \tag{2.21}$$

With the trigonometric relations $\cos(\alpha)\cos(\beta) = 0.5[\cos(\alpha+\beta)+\cos(\alpha-\beta)]$

and $\cos(\alpha)\sin(\beta) = 0.5[\sin(\alpha+\beta)-\sin(\alpha-\beta)]$, the result is obtained in the desired form:

$$\begin{aligned} v_{PM}(t) &= \hat{V}_c \cdot \{J_0(\eta)\cdot\cos(\omega_c t) \\ &\quad -J_1(\eta)\cdot[\sin(\omega_c + \omega_m)t + \sin(\omega_c - \omega_m)t] \\ &\quad -J_2(\eta)\cdot[\cos(\omega_c + 2\omega_m)t + \cos(\omega_c - 2\omega_m)t] \\ &\quad +J_3(\eta)\cdot[\sin(\omega_c + 3\omega_m)t + \sin(\omega_c - 3\omega_m)t] \\ &\quad + \ldots\} \end{aligned} \tag{2.22}$$

$$v_{PM}(t) = \hat{V}_c \sum_{n=-\infty}^{\infty} J_n(\eta)\cos\left[\omega_c t + n\left(\omega_m t + \frac{\pi}{2}\right)\right] \tag{2.23}$$

Therefore, the spectrum of an angle-modulated carrier with a sinusoidal modulation signal consists of the following components:

- carrier frequency f_c with the amplitude $J_0(\eta)\hat{V}_c$, as well as an infinite number of
- side-band frequencies $f_c + nf_m$ and $f_c - nf_m$ with the amplitudes $J_n(\eta)\hat{V}_c$

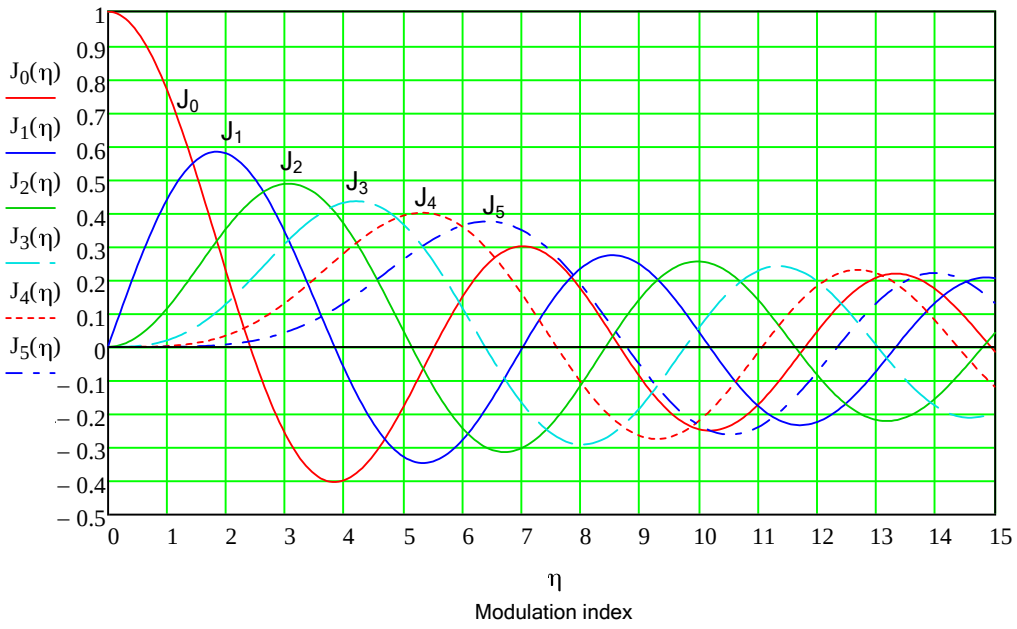

Fig. 2-2: Bessel functions $J_n(\eta)$ of first kind and order n

Roots of the Bessel functions

For certain phase deviations $\Delta\varphi_c$ (or modulation index η) the Bessel functions have roots. These can for example be used in measurement engineering for the precise determination of the modulation indexes.

Order n	Spectral line	Modulation index η			
		1st Root	2nd Root	3rd Root	4th Root
0	Carrier	2.405	5.520	8.654	11.792
1	1st Sideband	3.832	7.016	10.137	13.324
2	2nd Sideband	5.136	8.417	11.620	14.796
3	3rd Sideband	6.380	9.761	13.015	16.223

Table 2-1: Roots of Bessel functions of first kind

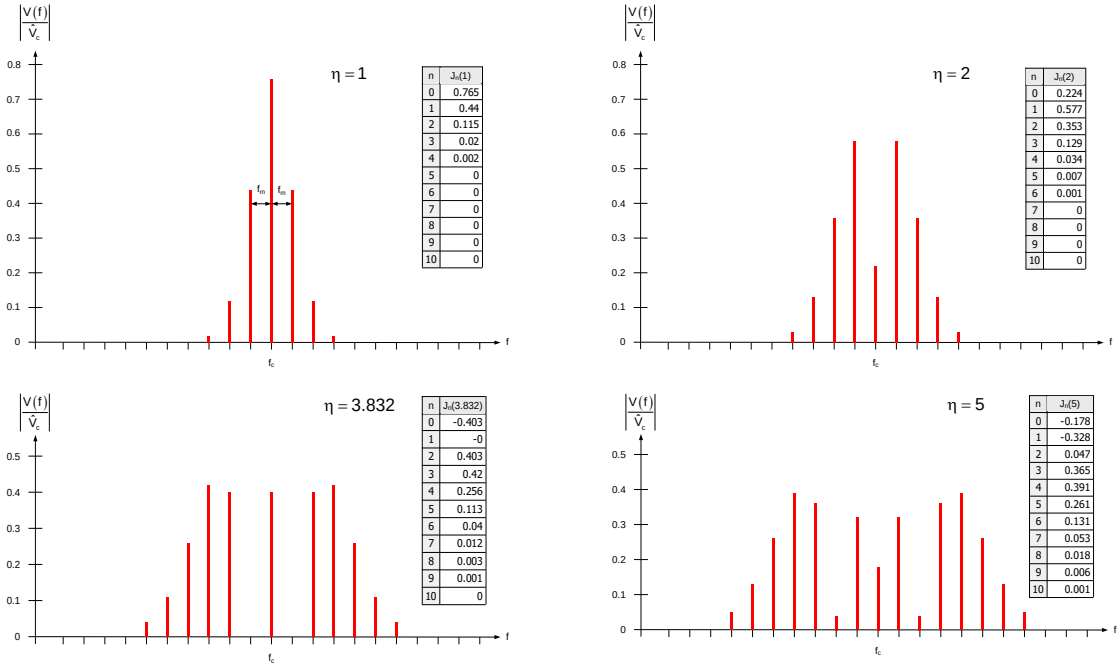

Fig. 2-3: Spectrum of angle modulated signals with different modulation index

The above spectrums show the following bandwidths for $|V(f)| \geq 0.1 \cdot \hat{V}_c$:

$\eta = 1$: $B_{PM} = 4 \cdot f_m$

$\eta = 2$: $B_{PM} = 6 \cdot f_m$

$\eta = 3.832$: $B_{PM} = 10 \cdot f_m$

$\eta = 5$: $B_{PM} = 12 \cdot f_m$

Particular attention should be paid to the roots of individual Bessel functions. For example, in the spectrum with $\eta = 3.832$, the function is $J_1(3.832) = 0$. Therefore, there are no spectral lines in a distance of f_m to the carrier.

Bandwidth of the angle modulation

When we examine the above examples and the Bessel functions, it is noticeable that starting from a certain ordinal number n, the spectral lines become smaller and smaller, and soon reaches values close to zero. Due to this, the spectrum, which theoretically has an infinite width, is practically limited to a finite value.

If only spectral lines with amplitudes $\geq 0.1 \cdot \hat{V}_c$ are taken into account, the bandwidth of an angle modulation signal can be represented as follows (Carson rule):

$$B_{PM} = 2 \cdot (\Delta f + f_m) = 2 \cdot f_m \cdot (1 + \eta) \tag{2.24}$$

If only spectral lines with amplitudes $\geq 0.01 \cdot \hat{V}_c$ are taken into account, the bandwidth will be:

$$B_{PM} = 2 \cdot (\Delta f + 2f_m) = 2 \cdot f_m \cdot (\eta + 2) \tag{2.25}$$

Another common definition for the bandwidth is the frequency range, which contains $\geq 99\%$ of the total power.

In the case of very small phase deviations of $\eta \leq 0.3$, all values of the Bessel function with n>1 are smaller than 0.01 and the amplitude spectrum is hardly distinguishable from an AM signal. However, the phase spectrum shows a phase shift of -90° in the side frequencies. This case is often called narrow-band FM (NBFM):

NBFM: $\eta \leq 0.3 \quad \left|J_n(\eta)\right| \leq 0.01$ for $n > 1$ (2.26)

In contrast to this, an angle modulation with a large modulation index is called wide-band FM (WBFM).

A typical example for this is FM broadcasting with a maximum modulation frequency of 15 kHz and a deviation stipulated in the standard of $\Delta f = 75\text{kHz}$. Hence, the modulation index is

$\eta = \frac{\Delta f}{f_{m_{max}}} = \frac{75\text{kHz}}{15\text{kHz}} = 5$ and the bandwidth according to (2.24) is

$B_{FM} = 2 \cdot (15\text{kHz} + 75\text{kHz}) = 180\text{kHz}$

When the spectrum is calculated, there are 8 spectral lines with an amplitude of $> 0.1\hat{V}_c$ on each side of the carrier; thus, the bandwidth is $B_{FM} = 2 \cdot 8 \cdot 15\text{kHz} = 240\text{kHz}$.

For AM, the relation between the bandwidth B_{AM} and the modulation frequency f_m is

$$\frac{B_{AM}}{f_m} = 2 \tag{2.27}$$

For the angle modulation, the relation is always greater than 2

$$\frac{B_{PM}}{f_m} = 2(1 + \eta) \tag{2.28}$$

In the case of the angle modulation, the occupied bandwidth is always greater than with AM. It is subject to the modulation index η.

Power of angle modulation signals

As during angle modulation, the amplitude of the carrier is not changed, the total power just corresponds to the power of the unmodulated carrier.

$$P_{PM} = P_c = \frac{\hat{V}_c^2}{2 \cdot R} \tag{2.29}$$

The amplitude of the spectral line of the carrier frequency f_c is for modulated signals significantly smaller than the amplitude of an unmodulated carrier. Eventually however, all phasors of the spectrum are added to form the constant signal amplitude.

The sum of the powers of all spectral lines also equals the power P_{PM}.

$$P_{PM} = \frac{\hat{V}_c^2}{2 \cdot R} \sum_{n=-\infty}^{+\infty} J_n^2(\eta) \qquad \text{with} \qquad \sum_{n=-\infty}^{+\infty} J_n^2(\eta) = 1 \tag{2.30}$$

As angle-modulated signals have a constant amplitude, they can be amplified in a non-linear way without the generation of modulation distortions. This is a big advantage especially for high-power transmitters, because non-linear amplifiers can have a very high degree of efficiency.

Representation options for angle modulation

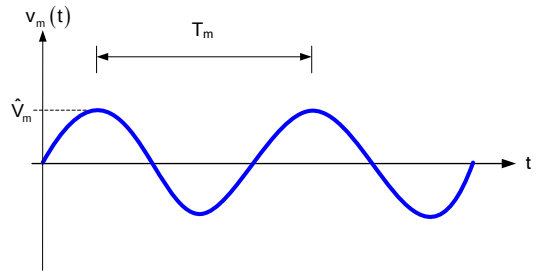

Fig. 2-4: Modulation signal in time domain

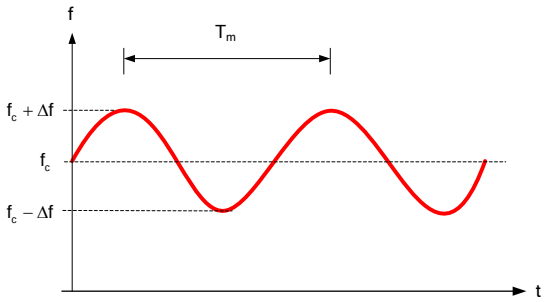

Fig. 2-5: Instantaneous frequency in time domain

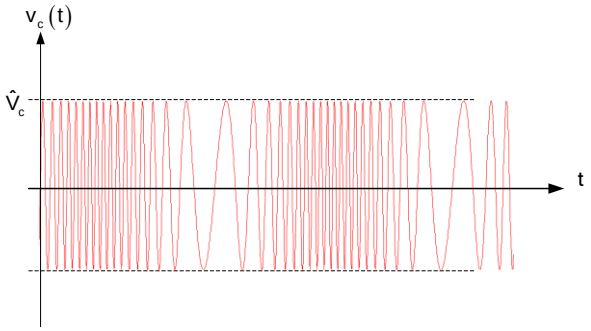

Fig. 2-6: Angle modulated signal in time domain

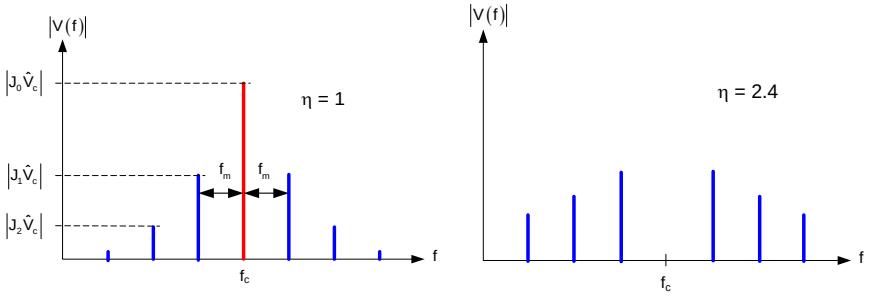

Fig. 2-7: Angle modulated signal in frequency domain

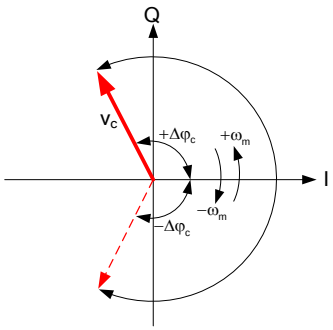

Fig. 2-8: Angle modulated signal in phase domain (pendulum phasor)

The phasor diagram below shows a PM signal with a very small modulation index. The component v_0 at f_c adds up to the resulting PM signal v_{PM} together with the two components v_{1a} und v_{1b} of the side frequencies.

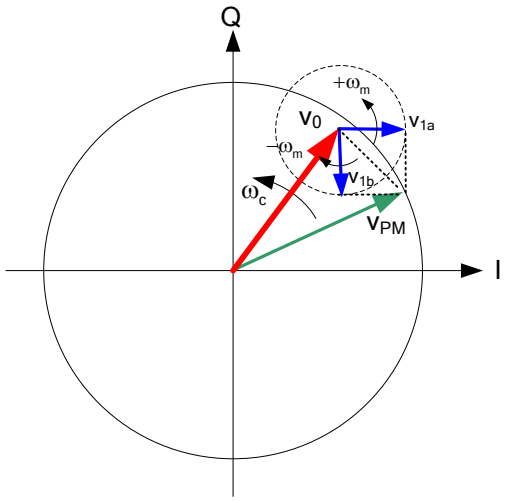

Fig. 2-9: Phasors for narrowband FM

The resulting phasor v_{PM} corresponds to the pendulum phasor in the pendulum phasor diagram. The other phasors however are harmonic waves, i.e. lines in the amplitude spectrum.

Phase modulation

The modulation signal influences the phase of the carrier. The phase angle of the carrier is changed by a value, which is proportional to the instantaneous value of the modulation signal.

From equation (2.6):

$$\varphi_{PM}(t) = \varphi_c(t) + \varphi_m(t) = \omega_c t + \Delta\varphi_c \cos(\omega_m t) \tag{2.31}$$

Hence, the following must apply

$$\varphi_{PM}(t) \sim v_m(t) \tag{2.32}$$

and

$$\Delta\varphi_c = \eta \sim \hat{V}_m \tag{2.33}$$

The phase deviation $\Delta\varphi_c$ is not subject to the modulation frequency, but it is proportional to the amplitude $\hat{V}_m$ of the modulation signal. The phase deviation $\Delta\varphi_c$ or modulation index η is the maximum deviation of the phase from the unmodulated carrier phase.

$$\Delta\varphi_c = \eta = k\hat{V}_m = \frac{\Delta f_c}{f_m} \qquad k = \text{ modulator constant} \tag{2.34}$$

The instantaneous frequency of the phase-modulated signal is determined by differentiation with respect to time (2.10) and (2.11)

$$f_{PM}(t) = \frac{1}{2\pi}\frac{d\varphi_{PM}(t)}{dt} = f_c - \Delta f_c \sin(\omega_m t) \tag{2.35}$$

$$\Delta f_c = k\hat{V}_m f_m \tag{2.36}$$

The frequency deviation Δf_c is proportional to the amplitude $\hat{V}_m$ of the modulation signal, but also proportional to the modulation frequency, due to the differentiation.

$$\Delta f_c \sim \hat{V}_m$$
$$\Delta f_c \sim f_m \tag{2.37}$$

Frequency modulation

The modulation signal influences the frequency of the carrier. The frequency of the carrier is changed by a value, which is proportional to the instantaneous value of the modulation signal.

From equation (2.11):

$$f_{FM(t)} = f_c + f_x(t) = f_c - \Delta f_c \sin(\omega_m t) = f_c - \eta\omega_m \sin(\omega_m t) \tag{2.38}$$

Hence, the following must apply

$$f_x(t) \sim v_m(t) \tag{2.39}$$

and

$$\Delta f_c \sim \hat{V}_m \tag{2.40}$$

The frequency deviation Δf_c is not subject to the modulation frequency, but it is proportional to the amplitude $\hat{V}_m$ of the modulation signal. The frequency deviation Δf_c is the maximum deviation of the frequency from the unmodulated carrier frequency f_c.

$$\Delta f_c = k\hat{V}_m = \Delta\varphi_c f_m \qquad k = \text{ modulator constant} \tag{2.41}$$

The instantaneous phase of the frequency-modulated signal is determined by means of integration with respect to time

$$\begin{aligned} \varphi_{FM}(t) &= \int \omega_{FM}(t)\,dt = \omega_c t + k\int v_m(t)\,dt \\ &= \omega_c t + \frac{\Delta f_c}{f_m}\sin(\omega_m t) = \omega_c t + \frac{k\hat{V}_m}{f_m}\sin(\omega_m t) \end{aligned} \tag{2.42}$$

$$\Delta\varphi_c = \frac{k\hat{V}_m}{f_m} \tag{2.43}$$

The phase deviation $\Delta\varphi_c$ is proportional to the amplitude $\hat{V}_m$ of the modulation signal, but also inversely proportional to the modulation frequency.

$$\begin{aligned} \Delta\varphi_c &\sim \hat{V}_m \\ \Delta\varphi_c &\sim \frac{1}{f_m} \end{aligned} \tag{2.44}$$

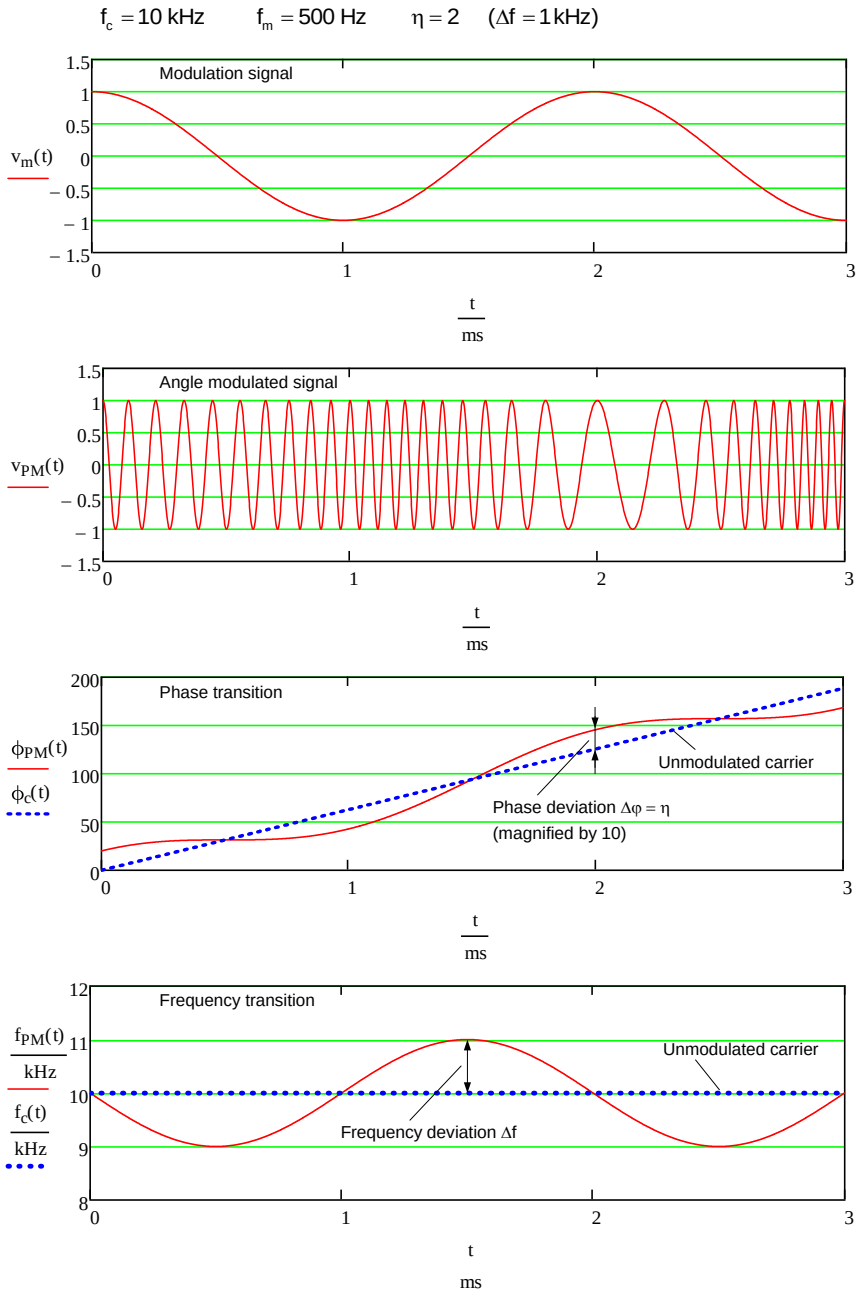

Fig. 2-10: Angle modulation with sinusoidal modulation signal

Fig. 2-11 shows a “Pendulum phasor diagram“ with the instantaneous position of the modulated carrier phasor with respect to the unmodulated carrier ($0^o \rightarrow$ "I").

The phase deviation $\Delta\varphi_c$ corresponds to the maximum deflection of the pendular phasor. The frequency deviation Δf_c is contained in the maximum oscillating speed $+\omega_{max}$ and $-\omega_{max}$.

For a constant modulation frequency f_m, the frequency deviation Δf_c and the phase deviation $\Delta\varphi_c$ or rather the modulation index η are closely linked to one another:

$$\Delta f_c = \eta \cdot f_m \qquad \text{bzw.} \qquad \eta = \Delta\varphi_c = \frac{\Delta f_c}{f_m} \tag{2.45}$$

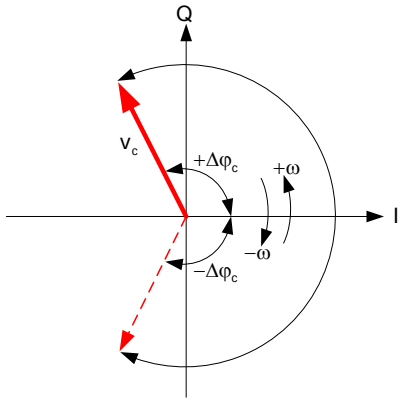

Fig. 2-11: Pendulum phasor of a phase modulated signal

In the case of a sinusoidal modulation signal with a constant frequency, frequency and phase modulation cannot be distinguished. Only if the modulation frequency is changed while the amplitude of the modulation signal remains constant, the differences become detectable:

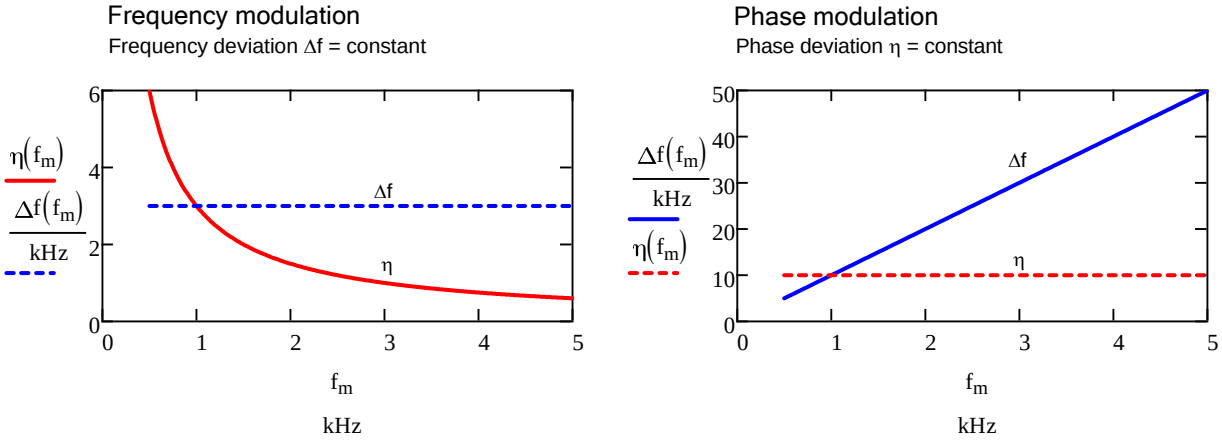

Fig. 2-12: Phase and frequency deviation for phase modulation and frequency modulation

2.2.2 Modulation Circuits

The angle modulation of a carrier can be effected as a phase modulation or as a frequency modulation. As in practice, frequency modulation can easier be realized than phase modulation, most of the practical circuits are frequency modulators. In this context, the oscillation frequency of an oscillator can be changed by the modulation signal. As frequency-determining elements in oscillators, LC resonant circuits, RC circuits and quartz or ceramic resonators are used. For sufficiently high frequencies, transmission line components can be used as resonators. The resonant frequencies can be influenced by means of controllable reactances as for example varicap diodes.

In the case of small frequency changes of <1% of the carrier frequency, a linear relation between the frequency and the control voltage can be achieved. Greater frequency deviations with good linearity can be obtained by means of frequency translation or frequency multiplication.

In the circuit in Fig. 2-13 the frequency modulation is generated on a high carrier frequency. In this process, even a greater frequency deviation remains small in relation to the carrier frequency so it fulfills the preconditions for linearity. The modulated signal is down-converted to a lower frequency.

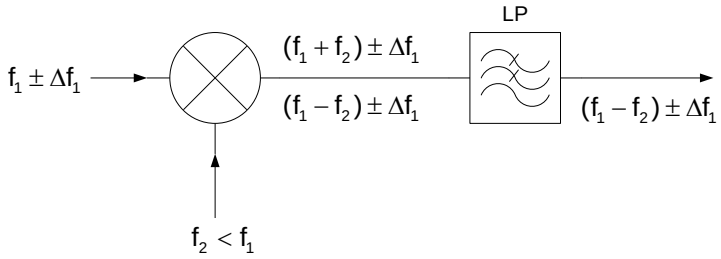

Fig. 2-13: Frequency modulator with downconverter

Another possibility, shown in Fig. 2-14, is frequency modulation with a small frequency deviation and a low carrier frequency with subsequent frequency multiplication. This procedure is often used, when the carrier frequency is generated by means of a quartz oscillator. This way, a very stable carrier frequency can be generated, whereas only a small frequency deviation of at most some 10ppm of the carrier frequency can be achieved.

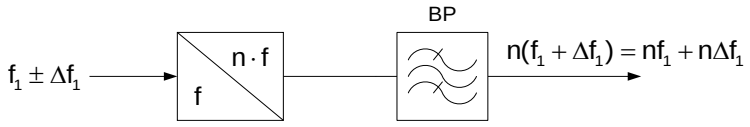

Fig. 2-14: Frequency modulator with multiplication

Frequency modulators

As FM modulator, mainly voltage controlled oscillators (VCO) are used. By means of the push-pull circuit of the two varicap diodes in Fig. 2-15, non-linearities of the second order can partially be compensated. The circuit in Fig. 2-16 uses a semi-rigid coax cable as resonator element with high Q. This way, a good frequency stability and low phase noise can be obtained with only little mechanical effort. In case of high requirements to frequency stability and stepped carrier frequencies, a synthesizer circuit with a PLL according to the basic circuit in Fig. 2-17 can be used. The modulation voltage is superimposed on the control voltage of the PLL and constitutes the control voltage of the VCO. The frequency of the VCO is proportional to its control voltage and produces the desired frequency modulation.

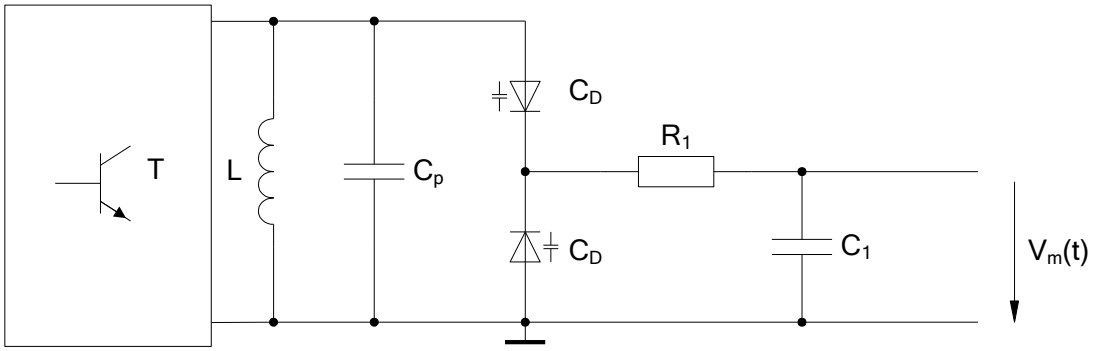

Fig. 2-15: LC-VCO using two varicap diodes

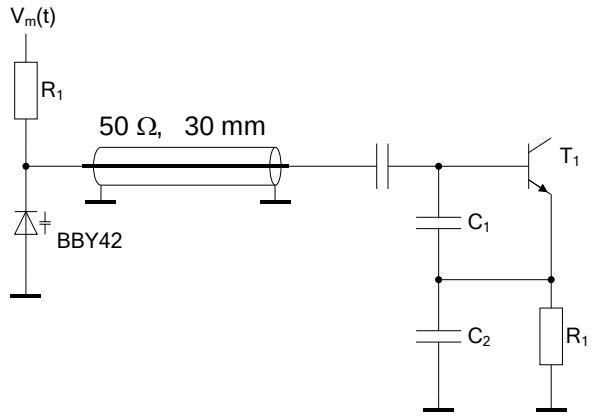

Fig. 2-16: VCO 350 – 550 MHz with coaxial line as resonator

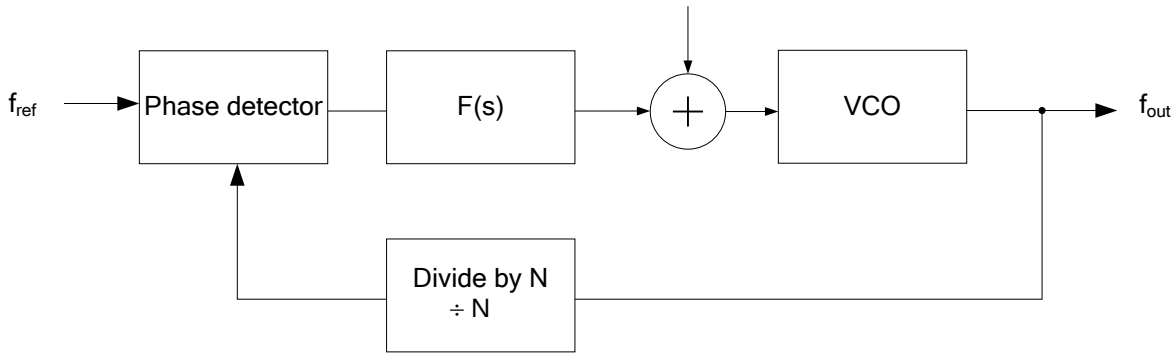

Fig. 2-17: Frequency modulator using Phase Locked Loop synthesizer

Phase modulators

For small phase deviations, voltage controlled band pass filters can be used as phase shifters. They allow for the phase modulation of carriers, which are generated by highly stable oscillators. The generated phase deviation can then be enhanced by means of frequency multipliers according to Fig. 2-14.

A simple method for the generation of a phase modulation is the quadrature modulator according to Fig. 2-18. With the multiplier, the modulation signal is multiplied with the carrier and generates a DSB signal with a suppressed carrier. To this signal, the carrier is added, which has been shifted by 90°. The remaining amplitude modulation within the resulting phase-modulated signal can be suppressed by means of a limiter.

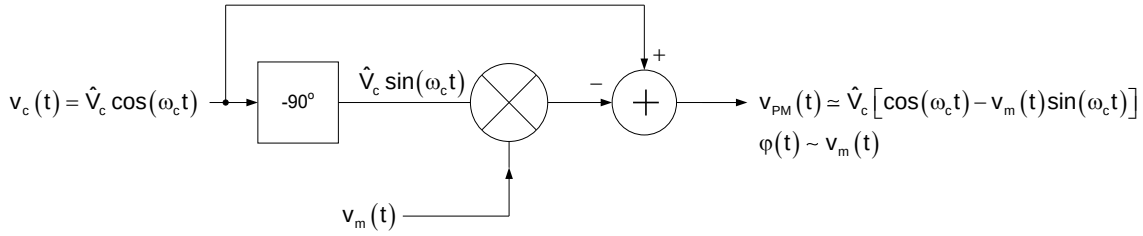

Fig. 2-18: Quadrature phase modulator

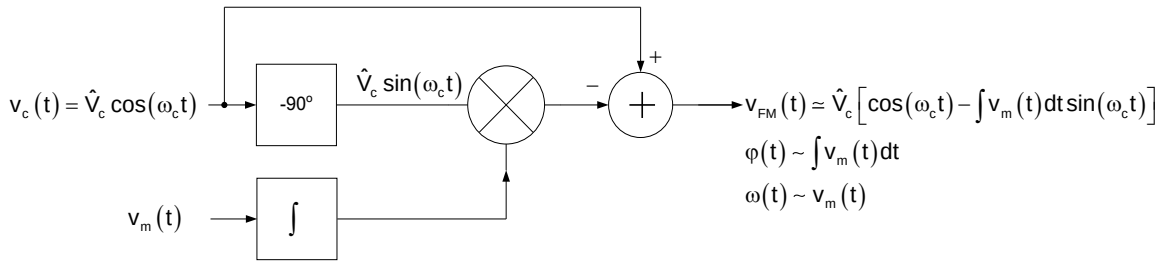

Fig. 2-19: Quadrature frequency modulator

Indirect frequency and phase modulation

FM and PM only differ in their modulation frequency response. Equation (2.35) shows that a phase modulation can be generated with a frequency modulator, if the modulation signal is differentiated. The differentiator can be realized as an RC high pass filter.

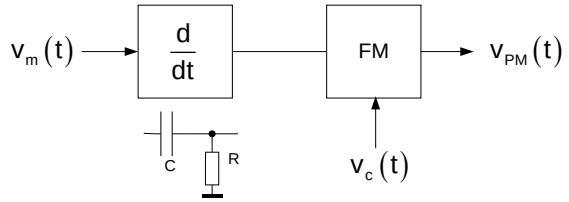

Fig. 2-20: Phase modulation using differentiator and frequency modulator

Vice versa, a frequency modulation can be generated using a phase modulator by means of the integration of the modulation signals, as shown in equation (2.42). The integrator can be realized by means of an RC low pass filter.

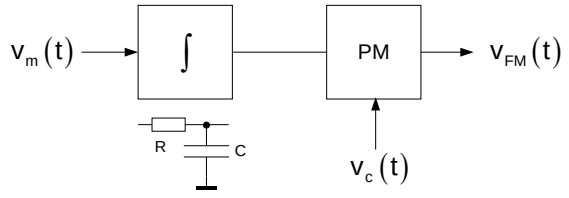

Fig. 2-21: Frequency modulation using integrator and phase modulator

Pre-emphasis and De-emphasis

There are several reasons for a decrease of the signal-to-noise ratio with the increasing frequency of the modulation signal during angle modulation:

- Most analog signals (music, speech) have higher frequencies with a lower power spectral density than medium or lower frequencies.
- At the demodulator output of the receiver, the noise power spectral density increases with the increasing modulation frequency.
- In the case of frequency modulation, the modulation index decreases with increasing modulation frequency and a constant frequency deviation. $\eta = \Delta f / f_m$

In order to improve the signal-to-noise ratio, the amplitudes of higher modulation frequencies are increased on the transmitter side (pre-emphasis) and decreased again on the receiver side (de-emphasis) so that a linear amplitude response is obtained across the entire system.

Pre-emphasis and de-emphasis are implemented by means of simple RC high- and low pass filters.

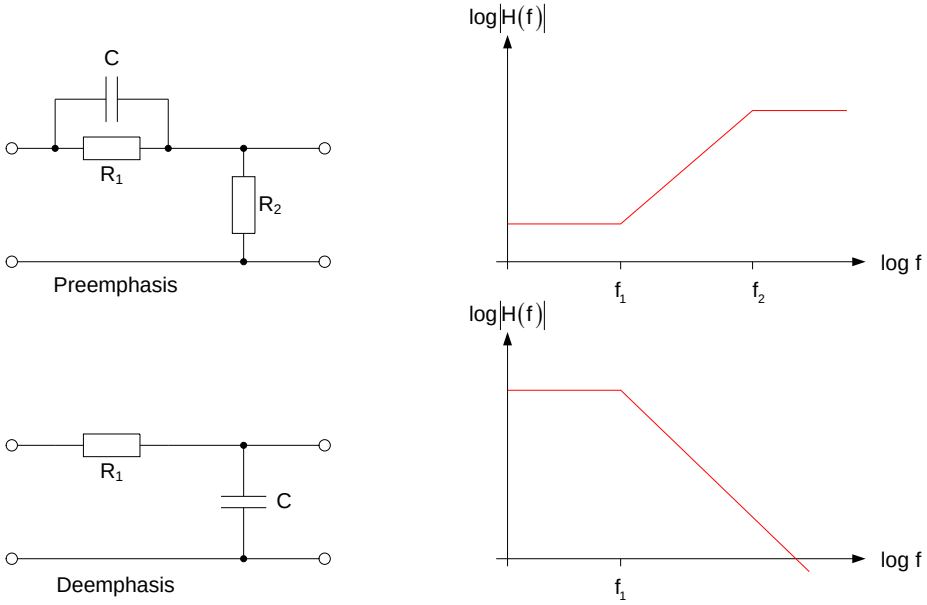

Fig. 2-22: Pre-emphasis and De-emphasis

The cutoff frequencies or time constants of the high- and low pass filters for broadcast systems have been defined in standards. In Europe, a time constant of $50\ \mu s$ is applicable for FM broadcasting. This corresponds to a cutoff frequency of 3.18kHz. (USA: $75\ \mu s$, 2.12kHz).

The following applies to the dimensioning of the RC members:

$$\tau = \frac{1}{2\pi f} \qquad f_1 = \frac{1}{2\pi R_1 C} \qquad f_2 = \frac{R_1 + R_2}{R_2} f_1$$

For f_2 a frequency higher than the highest audio frequency should be chosen.

By means of pre-emphasis and de-emphasis, an improvement of the signal-to-noise ratio on the receiver side of about 7dB can be obtained (Ref. [1]).

2.2.3 Demodulation Circuits

Angle-modulated signals contain the information in the frequency and phase oscillations, i.e. practically in the “zero crossings“. Their amplitudes in contrast are constant and therefore do not contain any information.

The interferences that are added during the transmission mainly consist of amplitude fluctuations. Therefore, it is generally reasonable to cut off a major part of these interferences with a limiter in front of the demodulation.

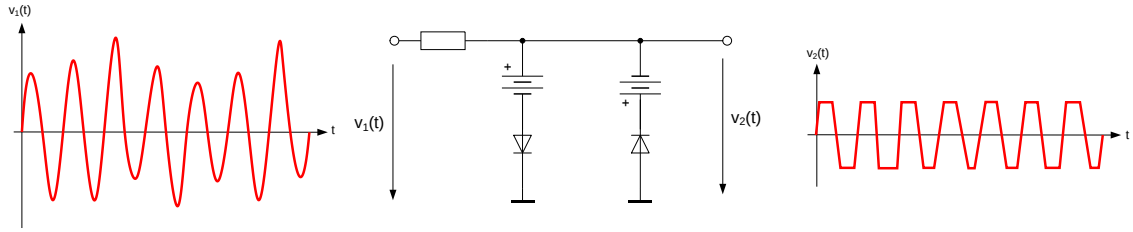

Fig. 2-23: Amplitude limiter

This is particularly necessary if the demodulation is carried out with an FM/AM converter (discriminator).

Slope discriminator

In the past, angle-modulated signals were practically only demodulated by means of a discriminator (FM/AM converter) with a subsequent AM demodulator.

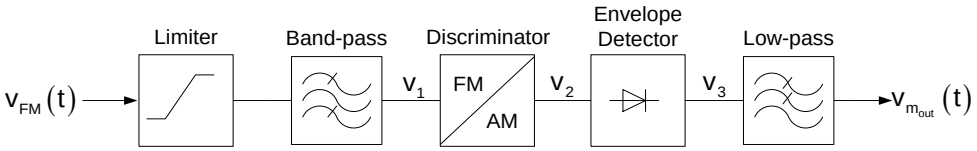

Fig. 2-24: Slope detector block diagram

As the simplest form of a discriminator, a differentiator can be used. Without taking into account the limiter and the band pass filter, the following applies:

$$v_{FM}(t) = v_1(t) = \hat{V}_c \cos\left[\omega_c t + k\int v_m(t)dt\right] = \hat{V}_c \cos\left[\omega_c t + \varphi(t)\right] \tag{2.46}$$

$$v_2(t) = \frac{dv_1(t)}{dt} = -\hat{V}_c\left[\omega_c + \frac{d\varphi}{dt}\right]\sin\left(\omega_c t + \varphi(t)\right) \tag{2.47}$$

$$v_3(t) = \hat{V}_c\left[\omega_c + \frac{d}{dt}\varphi(t)\right] = \hat{V}_c\omega_c + \hat{V}_c 2\pi k v_m(t) \tag{2.48}$$

$$v_{m_{out}}(t) = \hat{V}_c 2\pi k v_m(t) \qquad v_{m_{out}}(t) \sim v_m(t) \tag{2.49}$$

In practice, a band-pass filter with a slope that is as steep as possible, is used.

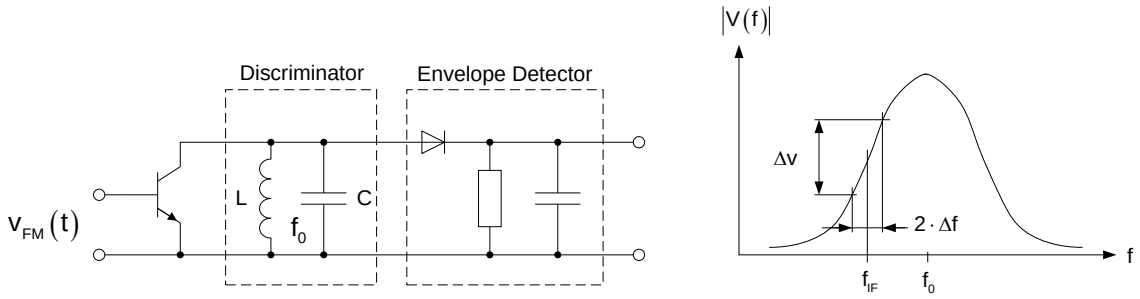

Fig. 2-25: Slope detector

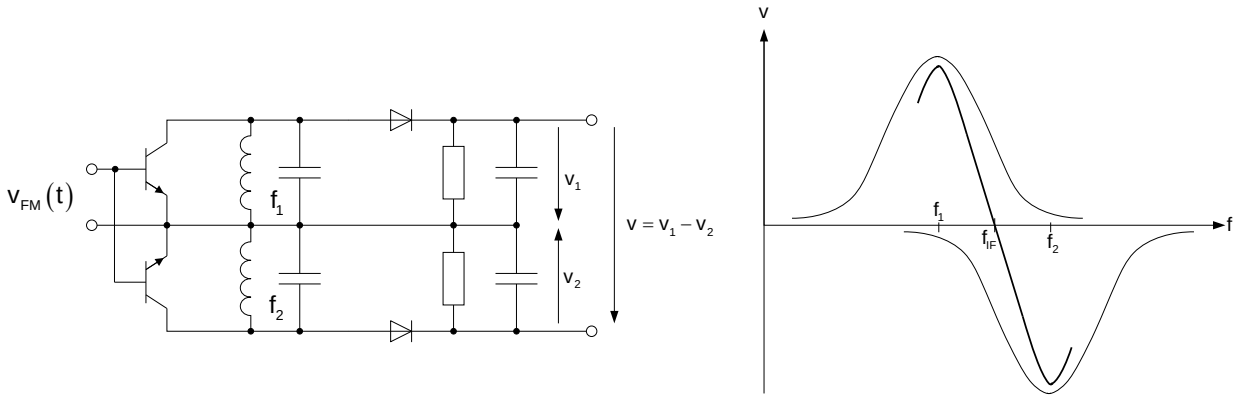

Fig. 2-26: Differential slope detector

For the differential slope detector in Fig. 2-26, two tuned circuits are used. One resonant frequency lies above, the other below the center frequency. The resulting characteristic curve of the detector has a larger bandwidth and an improved linearity.

Phase discriminator

The phase discriminator shown below has particularly good characteristics; it basically consists of an inductively coupled two-section band pass filter.

This basic circuit in Fig. 2-27 utilizes the frequency-dependent phase shifts that are generated inside the band pass filter, as shown in Fig. 2-28.

The phase discriminator is also known under the denomination Foster Seeley discriminator. A slightly modified circuit, in which the capacitive coupling with C_k was replaced by an inductive coupling, is called Riegger's circuit.

Despite its name, the phase discriminator is an FM demodulator.

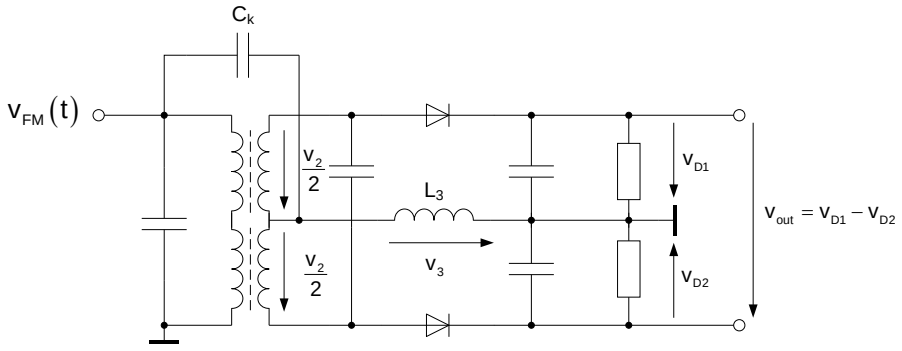

Fig. 2-27: Phase discriminator (Foster-Seeley)

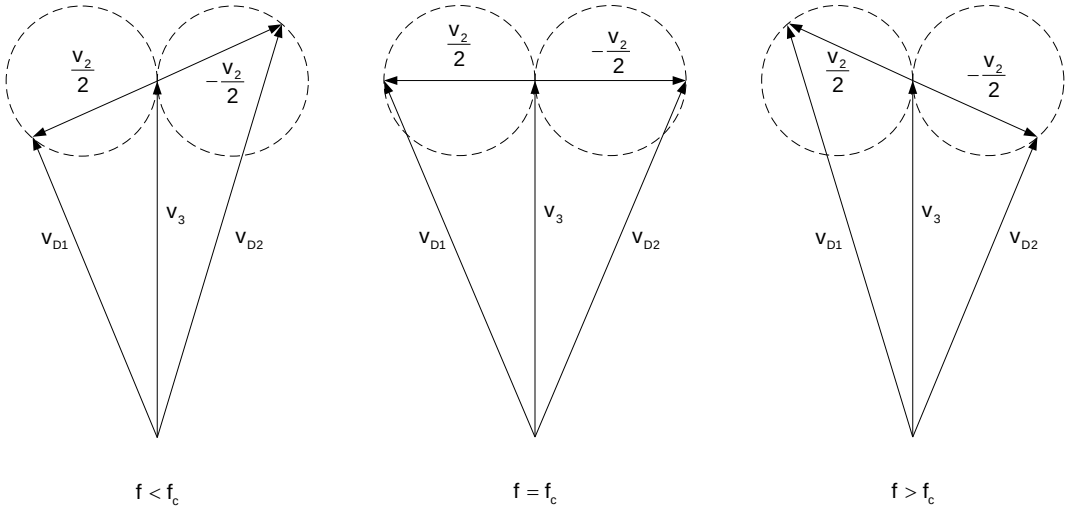

Fig. 2-28: Phasors for phase discriminator

These circuits have lost most of their relevance, as they cannot be implemented without large-volume and expensive LC circuits. In modern integrated circuit technology, the quadrature demodulator and the PLL demodulator have become the most accepted solutions. Both of them can be almost completely integrated, need only very few external elements and can generally be implemented without manual calibration.

PLL as FM demodulator

Today, phase locked loops (PLL) are often used for FM demodulation. The circuit blocks phase detector, low pass filter and VCO constitute a control loop, which synchronizes the VCO frequency with the angle-modulated input frequency.

Inside the phase detector, the two signals are compared. In case a phase error occurs, the VCO is readjusted accordingly.

As the VCO frequency is proportional to the control voltage, this control voltage concurrently corresponds to the frequency variations of the input signal, which equals an FM demodulation.

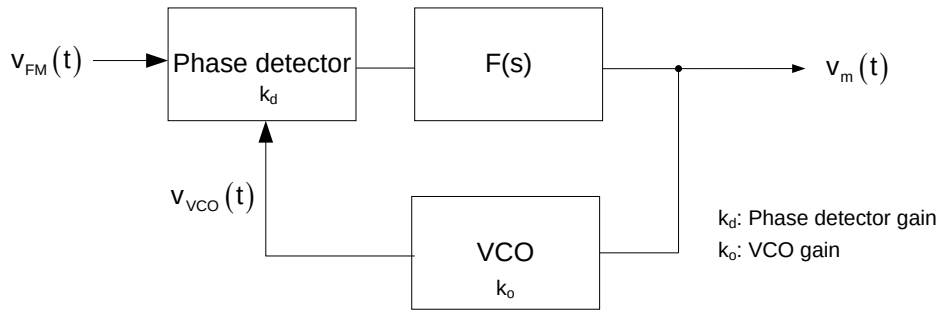

Fig. 2-29: PLL FM demodulator

$$v_{FM}(t) = \hat{V}_c \cos\left[\omega_c t + \Delta\varphi_1(t)\right]$$
$$v_{VCO}(t) = \hat{V}_{VCO} \cos\left[\omega_{VCO} t + \Delta\varphi_{VCO}(t)\right] \quad (2.50)$$

In locked state with $\omega_c = \omega_{VCO}$, $v_m(t) = k_d \sin\left(\Delta\varphi(t)\right)$ applies

and for $\Delta\varphi(t) < \frac{\pi}{6}$ $\quad v_m(t) \approx k_d \Delta\varphi(t)$ (2.51)

With $\Delta\omega_c(t) \sim \Delta\omega_{VCO}(t) = k_o v_m(t)$,

$v_m(t) \sim \Delta f_c(t)$ applies (2.52)

Quadrature demodulator

For the quadrature demodulator, other names and variants are used as well: coincidence demodulator or product demodulator.
The basic circuit is shown in Fig. 2-30.

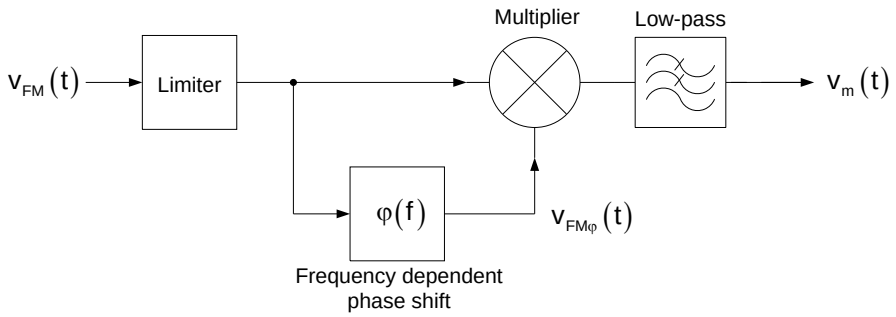

Fig. 2-30: Quadrature demodulator

The multiplier multiplies the frequency-modulated signal with the frequency-dependent phase-shifted signal.

$$v_{FM}(t) = \hat{V}_c \cos\left[\omega_c t + \frac{\Delta f}{f_m}\cos\left(\omega_m t\right)\right]$$
$$v_{FM\varphi}(t) = \hat{V}_c \cos\left[\omega_c t + \frac{\Delta f}{f_m}\cos\left(\omega_m t + \varphi(f)\right)\right] \quad (2.53)$$

After the multiplication and low-pass filtering, the following applies:

$$v_m(t) = \hat{V}\cos\left(\varphi(f)\right) \text{ and with } \varphi(f) = \frac{\pi}{2} \pm \Delta\varphi(f)$$

$$v_m(t) = \pm\hat{V}\sin\left(\Delta\varphi(f)\right) \tag{2.54}$$

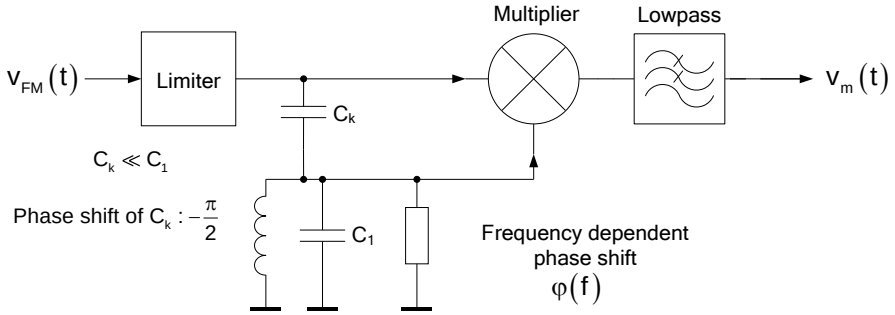

Fig. 2-31: Circuit for frequency dependent phase shift

WM modulators and demodulators with DSP

Today, modulators and demodulators are often implemented with digital signal processors (DSP). In a DSP modulator, the modulation signal is digitized, then the WM signal is calculated and is output through a D/A converter. Vice-versa, a DSP demodulator digitizes the RF or IF signal and calculates the modulation signal, which is then also output through a D/A converter.

2.2.4 Stereo Broadcast System

When stereo broadcasting was introduced in 1961, a system was chosen, which allowed for the continued use of mono receivers. The parameters that had been defined for mono systems, as for example the maximum frequency deviation, the frequency range of the modulation signal, the channel spacing and others had to be maintained. Today, a standard system defined by the regulatory authorities FCC (Federal Communications Commission) and CCIR (Comité Consultatif International des Radiocommunications) is used. In this system, a sum signal of the right and left audio signal $s_L(t) + s_R(t)$ and a difference signal $s_L(t) - s_R(t)$ is transmitted. On the receiver side, the original audio signals of the right and left channel are recovered by adding and subtracting the two signals.

$$\left[s_L(t) + s_R(t)\right] + \left[s_L(t) - s_R(t)\right] = 2 \cdot s_L(t)$$
$$\left[s_L(t) + s_R(t)\right] - \left[s_L(t) - s_R(t)\right] = 2 \cdot s_R(t)$$

The stereo system uses a frequency multiplex method with spectrum shown in Fig. 2-32. This “stereo multiplex signal” (MPX) or composite baseband contains the sum signal $s_L(t) + s_R(t)$, which is maintained with its original frequency and therefore constitutes a signal that is compatible for mono receivers. In addition, the difference signal $s_L(t) - s_R(t)$ is modulated on a 38kHz subcarrier with double sideband and suppressed carrier DSB-SC. The carrier is suppressed to a value of $\leq 1\%$. In order to facilitate the recovery of the carrier for demodulation with the correct phase in the receiver, a pilot tone of 19kHz is added, which is derived as a phase locked signal from the 38kHz carrier. Its amplitude is 10% of the maximum value of the multiplex signal.

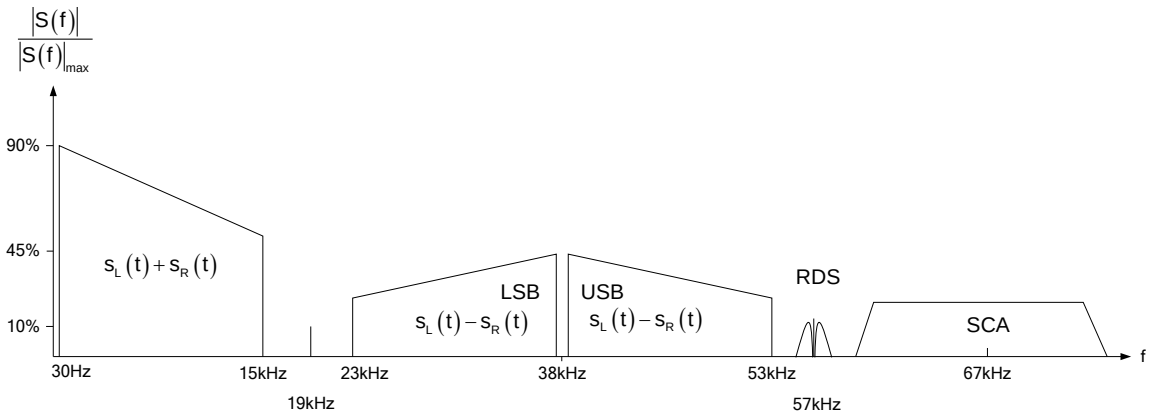

Fig. 2-32: Spectrum of the stereo composite baseband signal (Multiplex signal)

Other services as for example ARI (Autofahrer Rundfunk Information – broadcast system for traffic information), RDS (Radio Data System) and SCA (Subsidiary Communications Authorization) have been added in the course of time.

ARI: This system enables the activation of muted devices by means of an “announcement switching“ (Durchsagekennung – DK). The volume is increased and the device switches from any other audio source to the news announcement. ARI was introduced in 1975 and operated in Europe until 2005. From 1988, it was operated in parallel with the new RDS system.
A phase locked carrier with 57kHz, which is linked to the pilot tone, is amplitude-modulated with one of 6 possible frequencies in a range from 23 to 54Hz. The degree of modulation is 60%. These frequencies are used to distinguish different geographical areas. During the news announcement, the carrier is additionally amplitude-modulated with 125Hz and a modulation degree of 30% for the announcement switching (DK). All of the modulation frequencies can be derived from the pilot tone with an integer divisor.

RDS: With this system, a lot of additional information can be transmitted with digital data packages. RDS is defined in the standard EN 62106. The most important information being transmitted includes: Program Identification PI, Program Service Name PS, Alternative Frequency AF, Traffic Program TP, Traffic Announcement TA, Radio Text RT, Clock Time CT, Traffic Message Channel TMC, Enhanced Other Network EON.
The system uses a 57kHz carrier, which is in quadrature to the ARI carrier. This way, the parallel operation of ARI and RDS is possible. The bit rate of the RDS data is 1187.5bit/s. This data is Manchester-coded and filtered with a root cosine filter with $\alpha = 1$. With this signal, the 57kHz carrier is modulated with a binary phase shift keying with a symbol rate of 2375 Symbol/s. The RDS data is packed in data blocks of 26 bit. Each block contains 16 data bits and is completed by 10 check bits for the detection and correction of errors. 4 blocks are combined to form a group with 104 bit. Information regarding the group types and the coding can be found in the standard EN 6106.
The RDS signal should have a frequency deviation of 4kHz in the frequency-modulated signal.

SCA: Is mainly used in Canada and the USA for the transmission of additional information as stock market reports, background music, foreign language programs, etc. One or more carriers within a frequency range of 60kHz to 100kHz are modulated with the information. A common application is a frequency-modulated carrier for the transmission of background music in shopping centers.

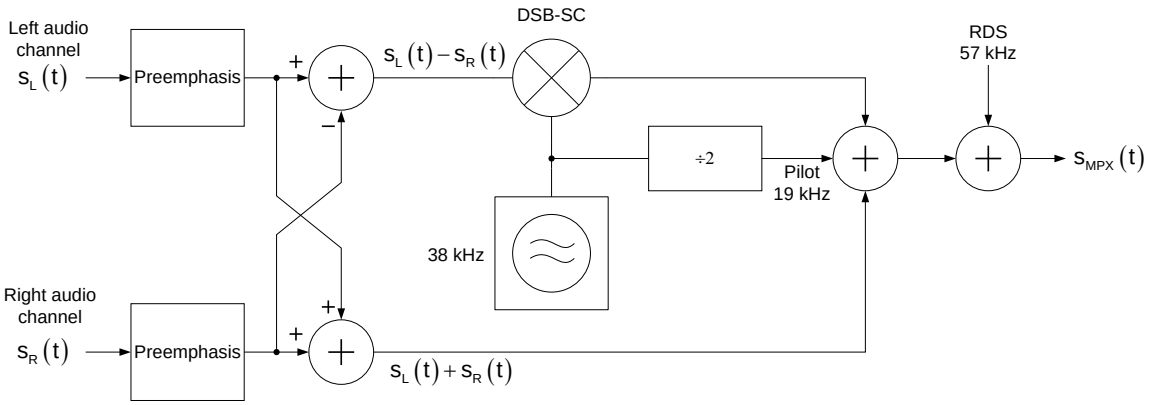

Fig. 2-33: Stereo coder block diagram

The complete baseband signal (MPX) is fed to the FM modulator of a transmitter. In order to limit the bandwidth of the modulated stereo signal, which could become too large due to the larger bandwidth of the baseband (57kHz without SCA in comparison to 15kHz with mono), the maximum frequency deviation for stereo was reduced from 75kHz to 67.5kHz. According to Carson (2.24), the bandwidth of the frequency-modulated stereo signal would then be

$$B = 2(67.5\ \text{kHz} + 57\ \text{kHz}) = 249\ \text{kHz}$$

in comparison to 180 kHz with the mono signal.

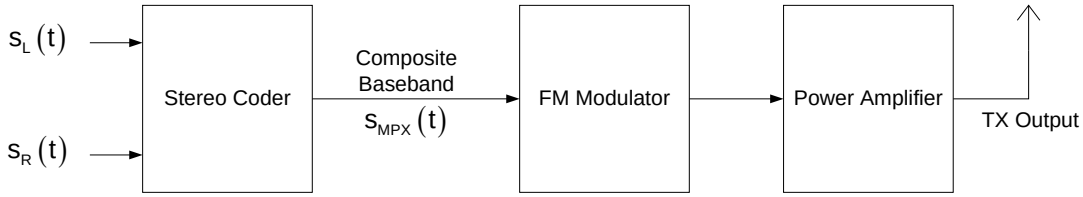

Fig. 2-34: Stereo transmitter

In the receiver, the first step is to recover the multiplex signal by means of an FM demodulator. For decoding the stereo multiplex signal and recovering the left and right audio signals, there are different solutions.

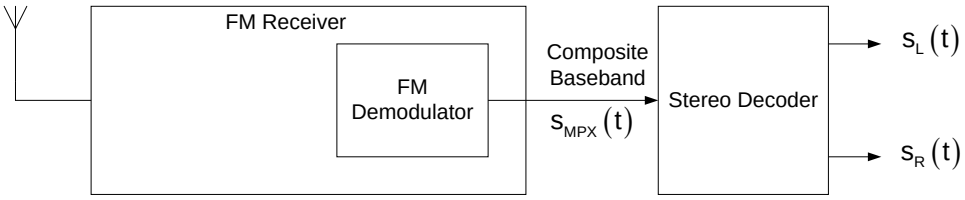

Fig. 2-35: Stereo receiver

Matrix decoder:

The sum signal $s_L(t) + s_R(t)$ is recovered by means of a low pass with a cut-off frequency of 15kHz. By means of a band pass filter from 23 to 53kHz, the DSB signal is recovered and demodulated in a synchronous demodulator by multiplication with the reconstructed carrier. After 15kHz low pass filtering, the difference signal $s_L(t) - s_R(t)$ is available. By adding and subtracting inside a resistor matrix network, the left and right audio signal is recovered.

The 38kHz carrier can be recovered by doubling the frequency of the pilot tone or by means of a PLL circuit.

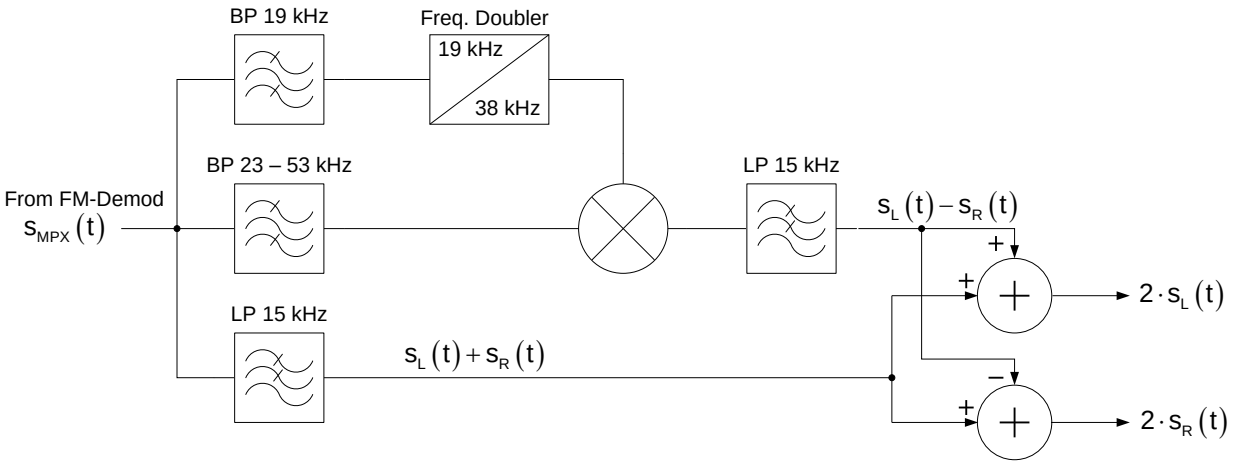

Fig. 2-36: Matrix stereo decoder

Envelope decoder:

If the carrier is added to the multiplex signal, a signal according to Fig. 2-37 results.

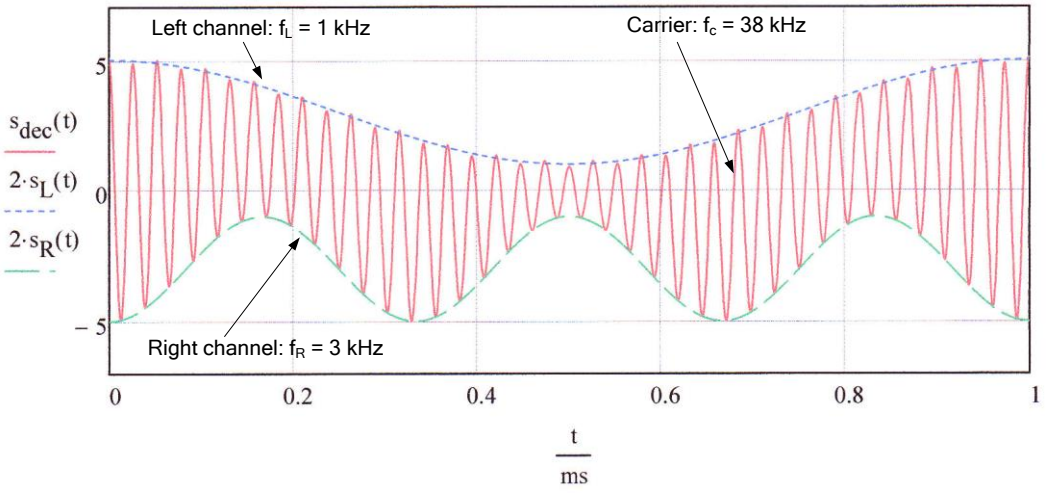

Fig. 2-37: Sum of multiplex signal and carrier

The upper envelope corresponds to the signal of the left channel and the lower envelope corresponds to the signal of the right channel. By means of simple envelope detectors, these signals can be demodulated.

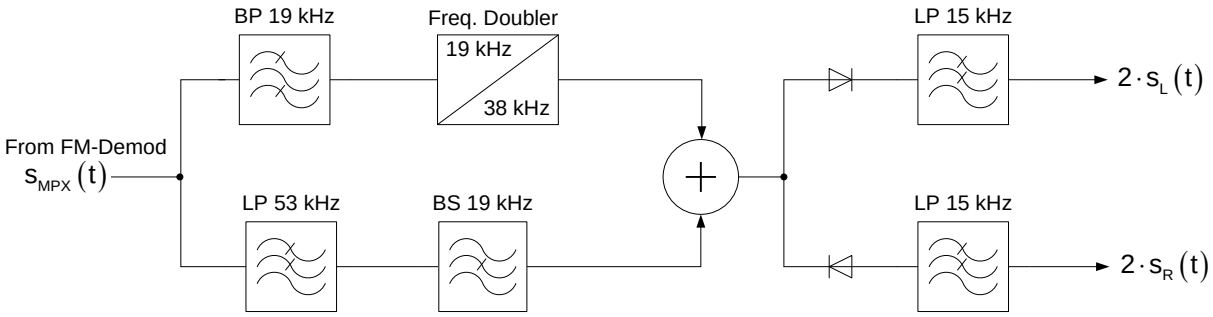

Fig. 2-38: Envelope-decoder

Switching decoder:

The multiplex signal shows that sampling of the signals at the instants of the carrier's maximum values produces the signal of the left channel and sampling at the instants of the carrier's minimum values produces the signal of the right channel.

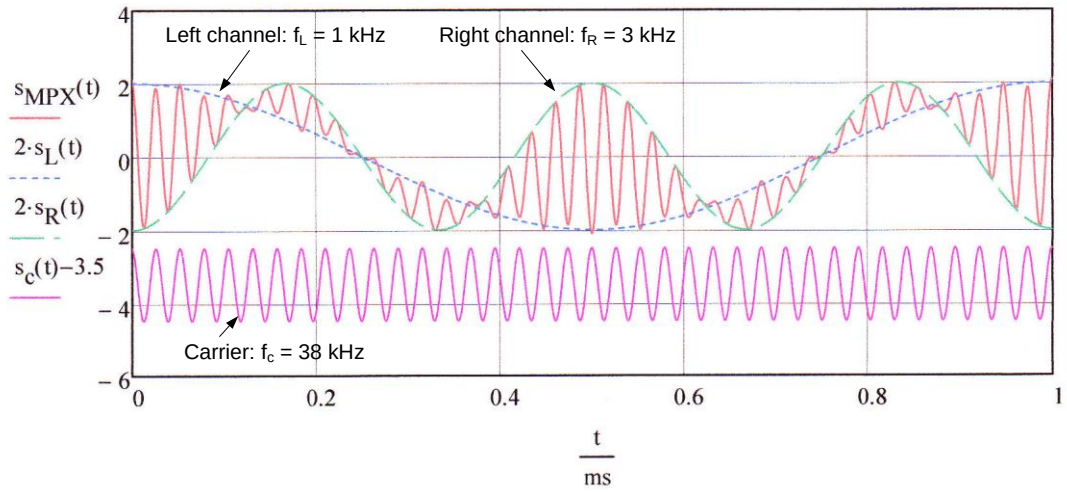

Fig. 2-39: Multiplex signal and 38 kHz-carrier

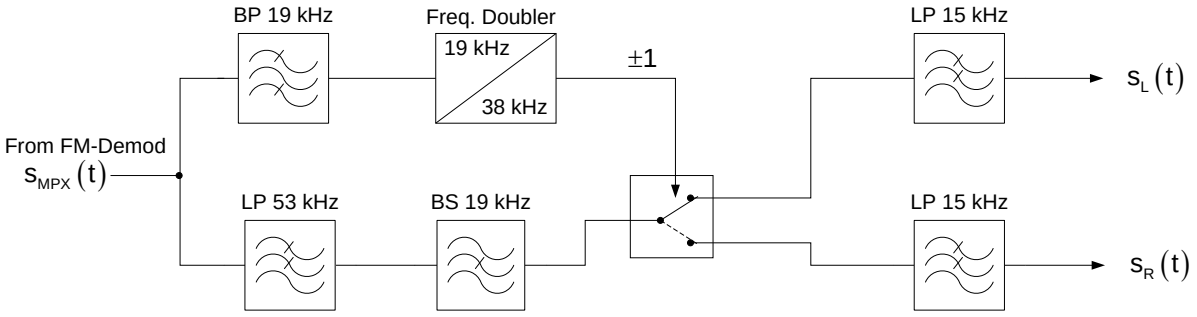

Fig. 2-40: Switching decoder

2.2.5 Distortion and noise behavior of FM

Distortions due to bandwidth limitation

If the phasor representation of the signal is used for angle-modulated signals, the sum phasor is at any point in time constituted by multiple phasors. As can be seen from equation (2.23), every spectral line $J_{-n}(\eta)$ to $J_{+n}(\eta)$ produces one phasor. The vectorial sum of all phasors at any point in time results in one point on a circle in the complex plane.

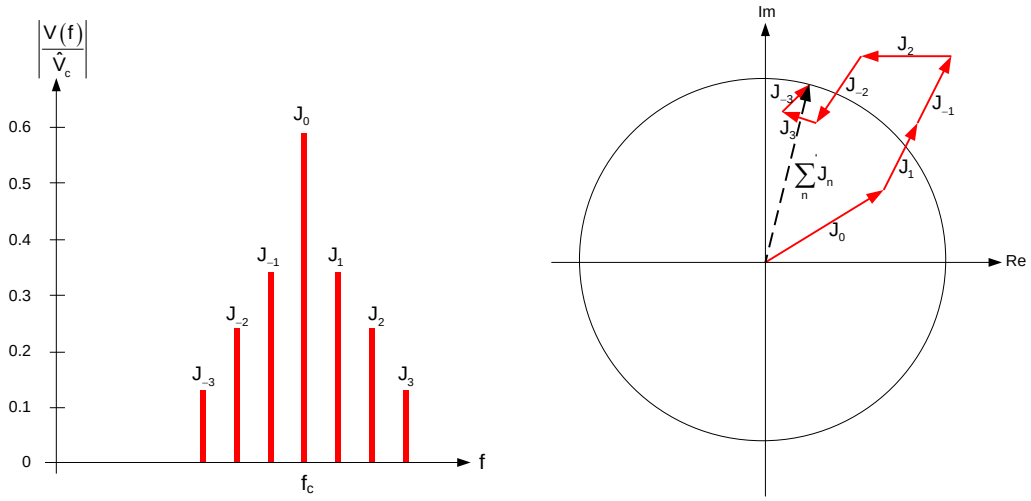

Fig. 2-41: Spectrum and phasor diagram of a frequency modulated signal

As shown in Fig. 2-41 the point of the sum phasor only moves on a circular locus, if all phasors of the spectral lines are present with the correct phasor length and phase. If there are linear distortions as amplitude response or group delay changes on the transmission path, the phasors of the spectral lines are distorted or are missing completely in case the bandwidth is too small. In this case, Fig. 2-42 shows that the instantaneous sum phasor has an incorrect length and an incorrect angle in comparison to the target value. As the ideal demodulator detects the phase $\varphi(t)$ of the signal, it produces an incorrect output signal. The distortions of the demodulated signal are non-linear.

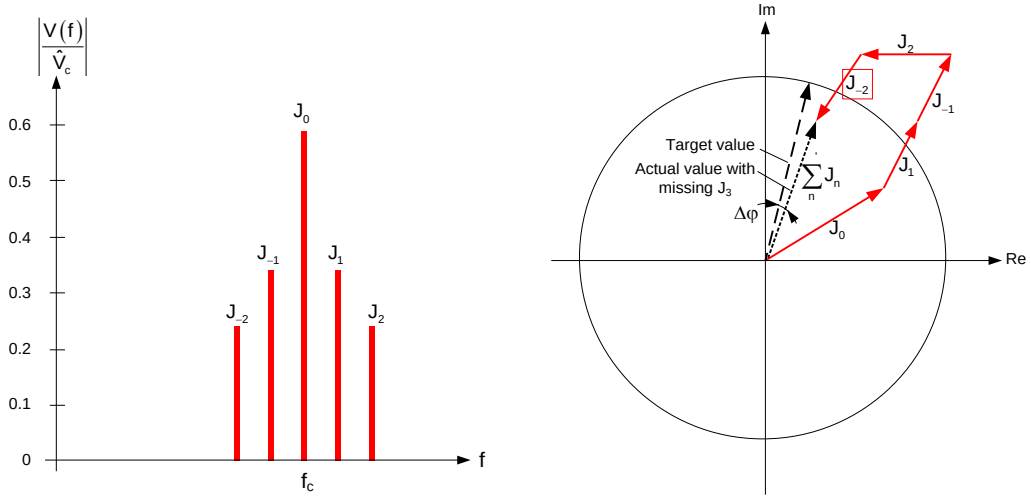

Fig. 2-42: Spectrum and phasor diagram of a frequency modulated signal with missing spectral lines due to insufficient bandwidth

New harmonics (harmonic distortion) are generated within the demodulated signal. The main cause of linear distortions within the system are mostly the intermediate frequency filters. If their bandwidth is insufficient, spectrum fractions of the signal are cut off; if the bandwidth is too large, the suppression of the adjacent channels will be too small. As a rule of thumb for the

necessary bandwidth for a required distortion factor of the demodulated signal, the following applies:

$$\text{THD} < 10\%: \quad B \geq 2\left(\Delta f + f_{m_{max}}\right) \qquad \text{(Carson Rule)}$$
$$\text{THD} < 1\%: \quad B \geq 2\left(\Delta f + 2f_{m_{max}}\right) \qquad \text{see also (2.24) and (2.25)} \qquad (2.55)$$

Here, the distortions of the demodulator have not been taken into account.

Noise

Similar to the case described in chapter 2.1.8, again, the signal and noise power is determined at the input and output of the demodulator and from this, the signal-to-noise ratios are calculated. Fig. 2-43 shows the block diagram with the FM demodulator.

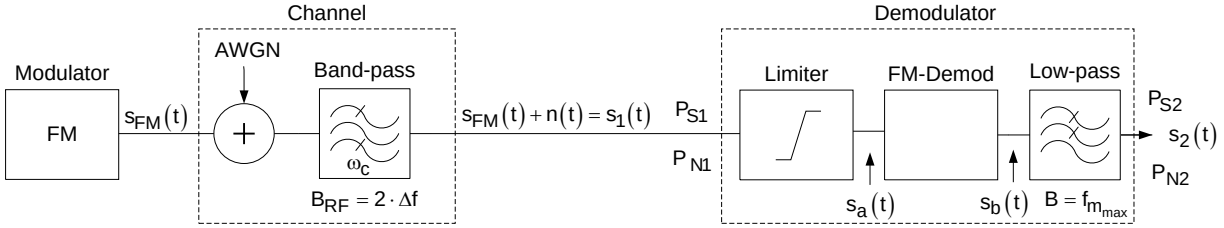

Fig. 2-43: Block diagram for noise analysis in FM systems

The time functions of the frequency and phase modulated signals are

$$s_{FM}(t) = S_c \cos\left[\omega_c t + k_{FM}\int s_m(t)dt\right] \qquad (2.56)$$

$$s_{PM}(t) = S_c \cos\left[\omega_c t + k_{PM} s_m(t)\right] \qquad (2.57)$$

k_{FM} and k_{PM} are modulator constants.

The signal power at the input of the demodulator is

$$P_{FM1} = P_{PM1} = P_{S1} = \frac{1}{2}S_c^{\,2} \qquad (2.58)$$

The RF bandwidth, which is relevant for the noise, can with (2.24)

$B_{RF} = 2\cdot(\Delta f + f_m)$ be further approximated with $B_{RF} \approx 2\Delta f$ for wideband FM with $\Delta f >> f_m$.

The noise power at the input of the demodulator is

$$P_{N1} = G_o B_{RF} \approx G_o 2\Delta f \qquad (2.59)$$

Hence, the signal-to-noise ratio at the input of the demodulator will be

$$\left(\frac{S}{N}\right)_1 = \frac{P_{S1}}{P_{N1}} = \frac{\frac{1}{2}S_c^{\,2}}{G_o B_{RF}} \approx \frac{\frac{1}{2}S_c^{\,2}}{G_o 2\Delta f} \approx \frac{S_c^{\,2}}{4G_o\Delta f} \qquad \left(\Delta f >> f_m\right) \qquad (2.60)$$

For the determination of the signal power at the output of the demodulator, it is assumed that the output signal is proportional to the instantaneous angular frequency $\omega(t)$. By means of the equation (2.56) and the differentiating function of the demodulator, the output signal of the FM demodulator can be determined.

$s_a(t) = k_D\left[\omega_c + k_{FM} s_m(t)\right]$ k_D: Demodulator constant

After the baseband low pass filter

$$s_a(t) = k_D k_{FM} s_m(t) \tag{2.61}$$

Accordingly, the signal power at the output

$$P_{S2} = k_D{}^2 k_{FM}{}^2 \overline{s_m{}^2(t)} \tag{2.62}$$

For the calculation of the noise power at the output, an unmodulated $(s_m(t) = 0)$ carrier and the additive noise are analyzed. It can be demonstrated that the noise is approximately independent of $s_m(t)$. For the purpose of noise analysis, the signal at the input of the demodulator is

$$\begin{aligned} s_1(t) &= S\cos(\omega_c t) + n(t) = S\cos(\omega_c t) + n_I(t)\cos(\omega_c t) - n_Q(t)\sin(\omega_c t) \\ &= \left[S + n_I(t)\right]\cos(\omega_c t) - n_Q(t)\sin(\omega_c t) \end{aligned} \tag{2.63}$$

The phasor diagram of this signal shows Fig. 2-44.

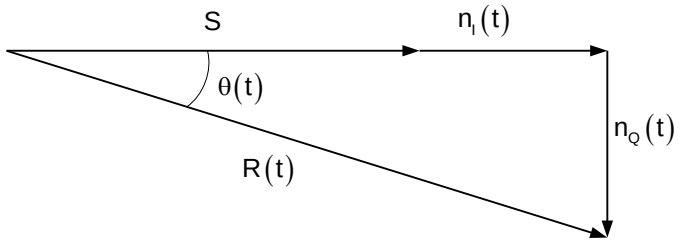

Fig. 2-44: Phasor diagram of $s_1(t)$, Eq. (2.63)

The envelope $R(t) = \sqrt{\left[S + n_I(t)\right]^2 + n_Q{}^2(t)}$ is not relevant for demodulation as all amplitude changes are removed by the limiter.

The phase $\theta(t)$ is

$$\theta(t) = \tan^{-1}\frac{n_Q(t)}{S + n_I(t)} \tag{2.64}$$

If it is assumed that the examined signal-to-noise ratio is large, the following applies: $|n_I(t)| << S$ and $|n_Q(t)| << S$.

With the approximation $\tan\theta \approx \theta$ for small θ, the following applies

$\theta(t) \approx \frac{n_Q(t)}{S}$, and the equation is

$$s_1(t) \approx S\cos\left(\omega_c t + \frac{n_Q(t)}{S}\right) \tag{2.65}$$

The output signal of the FM demodulator (differentiating circuit), will therefore be

$$s_b(t) = k_D \frac{1}{S}\frac{dn_Q(t)}{dt} \tag{2.66}$$

The power spectral density of the noise $n_Q(t)$ is G_o within the frequency range $-\frac{B_{RF}}{2} < f < \frac{B_{RF}}{2}$.

The differentiation of a signal corresponds to its transmission through a network with the transfer function $H(j\omega) = j\omega$.

For the FM demodulator, $H(j\omega) = j\frac{k_D\omega}{S}$ applies, and therefore $|H(j\omega)|^2 = \frac{k_D{}^2\omega^2}{S^2}$

The noise power spectral density at the output of the FM demodulator is

$$G_{FM_b}(f) = G_o \left|H(j\omega)\right|^2 = G_o \frac{k_D{}^2 \omega^2}{S^2} \tag{2.67}$$

The noise power spectral density $G_{FM_b}(f)$ is proportional to the square value of the frequency.

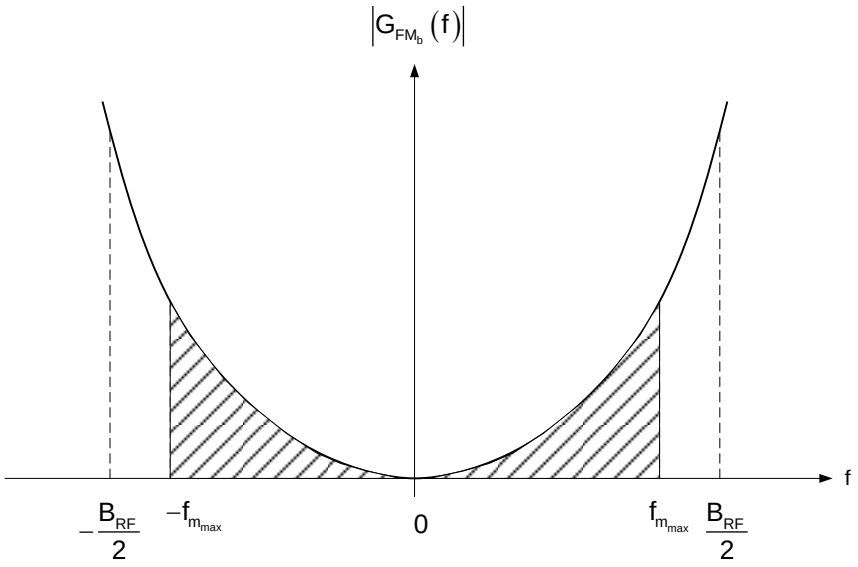

Fig. 2-45: Noise power spectral density at demodulator output

The low pass filter behind the FM demodulator has a cut-off frequency of $f_{m_{max}}$. The noise power at the output therefore corresponds to the shaded area in Fig. 2-45.

$$P_{N2} = \int_{-f_{m_{max}}}^{+f_{m_{max}}} G_{FM_b}(f)\,df = \frac{k_d{}^2 G_o}{S^2} \int_{-f_{m_{max}}}^{+f_{m_{max}}} 4\pi^2 f_m{}^2 df = \frac{8\pi^2}{3} \frac{k_D{}^2}{S^2} G_o f_m{}^3 = \frac{2}{3} \frac{k_D{}^2}{S^2} G_o \frac{\omega_m{}^3}{2\pi} \tag{2.68}$$

With (2.62) and (2.68), the output signal-to-noise ratio is

$$\left(\frac{S}{N}\right)_2 = \frac{P_{S2}}{P_{N2}} = \frac{k_D{}^2 k_{FM}{}^2 s_m{}^2(t)}{\frac{8\pi^2 k_D{}^2 G_o f_m{}^3}{3S^2}} = \frac{3S^2 k_{FM}{}^2 s_m{}^2(t)}{8\pi^2 G_o f_m{}^3} \tag{2.69}$$

With a sinusoidal modulation signal $s_m(t)$, (2.61) will be

$$k_{FM} s_m(t) = 2\pi\Delta f \cos(2\pi f_m t)$$

and

$$k_{FM}{}^2 s_m{}^2(t) = \frac{4\pi^2 \Delta f^2}{2} = 2\pi^2 \Delta f^2 \qquad \text{inserted in (2.69) results in}$$

$$\left(\frac{S}{N}\right)_2 = \frac{3S^2 \Delta f^2}{4 G_o f_{m_{max}}{}^3} = \frac{3}{2}\left(\frac{\Delta f}{f_{m_{max}}}\right)^2 \frac{S^2/2}{G_o f_{m_{max}}} = \frac{3}{2}\eta^2 \frac{P_{S1}}{P_{N1}} = \frac{3}{2}\eta^2 \left(\frac{S}{N}\right)_1 \tag{FM(2.70)}$$

The same analysis with (2.57) for phase modulation results in

$$\left(\frac{S}{N}\right)_2 = \frac{1}{2}\eta^2\left(\frac{S}{N}\right)_1 \qquad \text{PM(2.71)}$$

Therefore, phase demodulation is inferior to FM by a factor 3 or by 4.8dB.

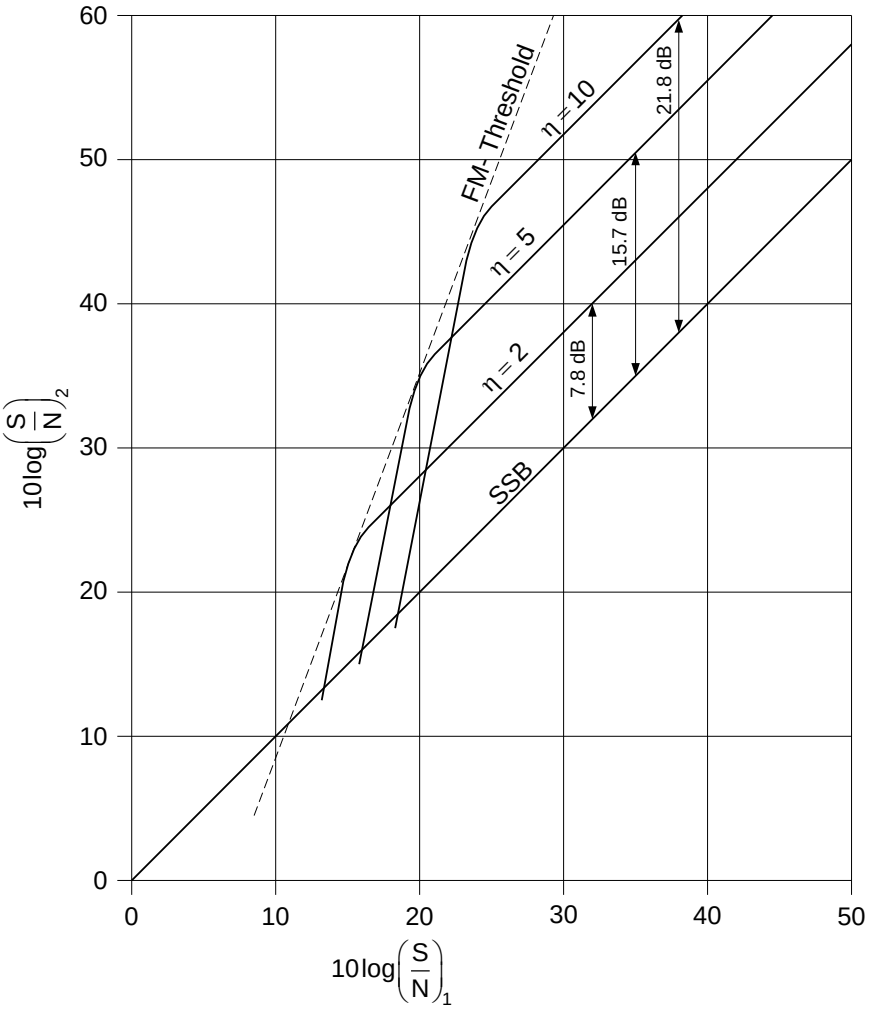

Fig. 2-46: Output S/N versus input S/N for FM

Fig. 2-46 shows the signal-to-noise ratios for FM demodulators. For the derivation of the equations, among other things, the approximations $\Delta f << f_m$ and $n(t) << s(t)$ have been used. The equations are therefore approximations for large modulation indexes η and large signal-to-noise ratio S/N. Numerical values are to be used with caution. Measurements of FM demodulators however show good agreement with these approximations. The distinct FM thresholds of FM demodulators show that below the threshold, the signal-to-noise ratio is steeply declining. Exact calculations of this characteristic were carried out by Stumpers [7] and Rice [8]. The threshold is a function of the modulation index η and is shifted to higher S/N values with an increasing η. In Ref. [1], it is shown that PLL demodulators have a 2 to 3dB lower threshold than discriminators.

Above the FM threshold, a significant modulation gain can be achieved with FM in comparison to SSB, however at the expense of a larger bandwidth. FM broadcast systems use a maximum audio frequency $f_{m_{max}}$ of 15kHz and a frequency deviation of 75kHz. The modulation gain $(S/N)_2 / (S/N)_1$ for SSB is 1 and for FM $\frac{3}{2}\eta^2 = \frac{3}{2}\left(\frac{75\text{kHz}}{15\text{kHz}}\right)^2 = 37.5 \triangleq 15.7\,\text{dB}$. With $B = 2(\Delta f + f_{m_{max}}) = 180\ \text{kHz}$ the bandwidth for FM is significantly larger than for SSB with 15kHz.

Below the FM threshold, the modulation gain rapidly declines and is even smaller for small S/N than for SSB.

Above the FM threshold, FM is superior to SSB with a modulation index of $\eta > \sqrt{\frac{2}{3}} = 0.82$.

Equation (2.67) shows that the noise power spectral density of the demodulated signal quadratically increases with the frequency. This way, the signal-to-noise ratio decreases with an increasing modulation frequency, while the amplitude of the modulation signal is constant. The pre-emphasis described in chapter 2.2.2 counteracts this effect.

Equation (2.68) shows that the noise power at the output of the demodulator is inversely proportional to the carrier power $S^2 / 2$. S is limited by the limiter and remains constant for input powers above the limiting value. Without an input signal, the FM demodulator produces a significant noise voltage at the output, which is reduced by an applied carrier. The noise reduction can also be used for measuring the sensitivity (minimum input signal) of an FM receiver. For analog radio systems, a noise reduction (quieting) value of 20dB was common.

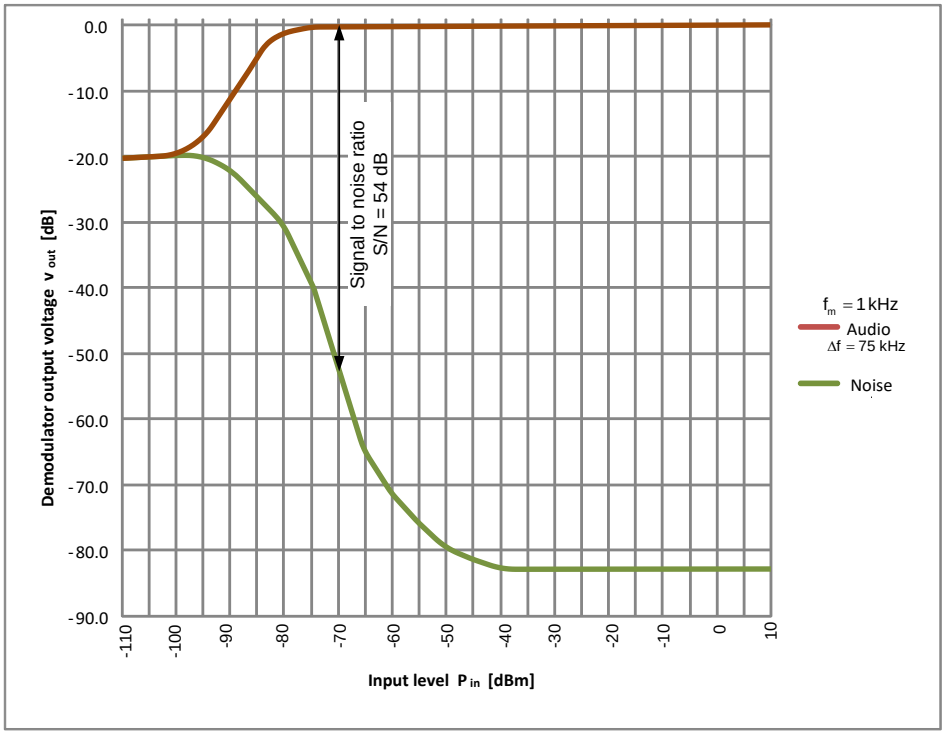

Fig. 2-47: Measured audio and noise output voltage versus input level of a high quality FM demodulator

2.3 References

[1] Taub, H., Schilling, D.L.: *Principles of communication systems*. McGraw-Hill, 2nd Edition 1986

[2] Kammeyer, K.D. : *Nachrichtenübertragung*. Vieweg+Teubner, 4. Auflage 2008

[3] Roppel, C.: *Grundlagen der digitalen Kommunikationstechnik*. Carl Hanser Verlag, 2006

[4] Ohm, J-R., Lüke, H.D.:*Signalübertragung*. Springer Verlag Berlin, 10. Auflage 2007

[5] Schwartz, M.: Information, Transmission, Modulation, and Noise. McGraw-Hill, 1980

[6] Zinke, O., Brunswig, H.: *Hochfrequenztechnik 2*, Springer Verlag Berlin, 5. Auflage 1999

[7] Stumpers, F.L.M.H.: *Theory of frequency modulation noise*. Proc. Inst. Radio Engrs. 36, 1948, 1081-1092

[8] Rice, S.O. : *Statistical properties of a sine wave plus random noise*. Bell Syst. Techn.J. 27, 1948, 109-157

[9] von Grünigen, D.Ch.: *Digitale Signalerarbeitung mit einer Einführung in die kontinuierlichen Signale und Systeme.* Carl Hanser Verlag, 5. Auflage 2014

[10] von Grünigen, D.Ch.: *Digitale Signalerarbeitung: Bausteine, Systeme, Anwendungen.* Fotorotar Print und Media, 2008

[11] Dellsperger, F.: *Passive Filter der Hochfrequenz- und Nachrichtentechnik.* Lecture Script, 2012